REPORT DOCUMENTATION PAGE	Form Approved OMB No. 0704-0188

1. AGENCY USE ONLY *(Leave blank)*	2. REPORT DATE	3. REPORT TYPE AND DATES COVERED
	14.Oct.98	THESIS

4. TITLE AND SUBTITLE
CHARACTERIZATIN STUDY OF CONVENTIONAL CHROMIUM FILMS, AMORPHOUS BRIGHT CHROMIUM DEPOSITED (ABCD) FILMS, N+ IMPLANTED ABCD FILMS AND THE PREPARATION OF ABCD FILMS USING

5. FUNDING NUMBERS

6. AUTHOR(S)
2D LT GONZALEZ RENE I

7. PERFORMING ORGANIZATION NAME(S) AND ADDRESS(ES)
UNIVERSITY OF FLORIDA

8. PERFORMING ORGANIZATION REPORT NUMBER

9. SPONSORING/MONITORING AGENCY NAME(S) AND ADDRESS(ES)
THE DEPARTMENT OF THE AIR FORCE
AFIT/CIA, BLDG 125
2950 P STREET
WPAFB OH 45433

10. SPONSORING/MONITORING AGENCY REPORT NUMBER
98-084

11. SUPPLEMENTARY NOTES

12a. DISTRIBUTION AVAILABILITY STATEMENT
Unlimited distribution
In Accordance With AFI 35-205/AFIT Sup 1

12b. DISTRIBUTION CODE

13. ABSTRACT *(Maximum 200 words)*

14. SUBJECT TERMS

15. NUMBER OF PAGES

16. PRICE CODE

17. SECURITY CLASSIFICATION OF REPORT	18. SECURITY CLASSIFICATION OF THIS PAGE	19. SECURITY CLASSIFICATION OF ABSTRACT	20. LIMITATION OF ABSTRACT

CHARACTERIZATION STUDY OF CONVENTIONAL CHROMIUM FILMS, AMORPHOUS BRIGHT CHROMIUM DEPOSITED (ABCD) FILMS, N^+-IMPLANTED ABCD FILMS AND THE PREPARATION OF ABCD FILMS USING PROPIONIC ACID AS AN ORGANIC ADDITIVE

By

RENE I. GONZALEZ

A THESIS PRESENTED TO THE GRADUATE SCHOOL
OF THE UNIVERISTY OF FLORIDA IN PARTIAL FULFILLMENT
OF THE REQUIREMENTS FOR THE DEGREE OF
MASTER OF SCIENCE

To Monica

ACKNOWLEDGEMENTS

I would like to thank Gar B. Hoflund, John T. Wolan and Charles K. Mount for their help, tutelage and support during my stay at the University of Florida. I value their friendship, and I am honored to have had the opportunity to work with them. I would also like to thank my parents and my fiancée, Monica, whom I love dearly.

TABLE OF CONTENTS

Abstract of Thesis Presented to the Graduate School
of the University of Florida in Partial Fulfillment of the
Requirements for the Degree of Master of Science

CHARACTERIZATION STUDY OF CONVENTIONAL CHROMIUM FILMS, AMORPHOUS BRIGHT CHROMIUM DEPOSITED (ABCD) FILMS, N^+-IMPLANTED ABCD FILMS AND THE PREPARATION OF ABCD FILMS USING PROPIONIC ACID AS AN ORGANIC ADDITIVE

By

Rene I. Gonzalez

May 1998

Chairman: Gar B. Hoflund
Major Department: Chemical Engineering

Electroplated chromium films are widely used and are extremely important in industrial processes because the films produced are hard, corrosion resistant, bright and have good adhesive properties. Unfortunately, the utilization of conventional Cr layers is limited to low-temperature applications (generally less than 50°C) because they soften at elevated temperatures. This problem has been overcome through the development of the amorphous bright chromium deposition (ABCD) method. In the ABCD method organic compounds containing -CHO or -COOH groups are added to the electroplating bath, and the bath is operated under different conditions than the conventional Sargent bath. The resulting ABCD films have exceptional properties compared to conventional Cr films. Most importantly, the hardness of ABCD films increases greatly either by annealing at fairly low temperatures for long periods (200°C for 48 hrs) or higher temperatures for shorter periods (600°C for 1/2 hr) thereby opening new application areas for Cr layers.

Since the hardness behavior of ABCD films is superior to that of conventional Cr films, it is important to understand the hardness behavior in terms of the chemical nature of

these films. Previous studies have shown that the Cr layers are quite complex compositionally and structurally and that both change significantly with sample treatment. Nevertheless, the hardness behavior seems to depend primarily upon annealing temperature. These facts suggest that the types of chemical species present and microstructural properties of ABCD films are important in determining their hardness behavior.

In this study scanning electron microscopy and scanning Auger microscopy have been used to examine both as-prepared and annealed ABCD and conventional Cr films. The data indicate large differences between the conventional and ABCD films with regard to surface morphology, the amounts and chemical forms of C present and the alterations which occur in the films during annealing.

The ABCD films annealed at 100 and 700°C and N^+ implanted have also been examined in this study using Auger electron spectroscopy (AES), ion scattering spectroscopy (ISS), X-ray photoelectron spectroscopy (XPS) and sputter depth profiling in order to determine the composition of the near-surface region and the chemical species present. Both N^+ implanting and annealing increase the hardness of ABCD films particularly in the near-surface region (outermost 200 nm) according to depth-sensitive Knoop hardness measurements. The near-surface hardness of the 100°C annealed and N^+ implanted ABCD film is 3280, and that of the 700°C annealed and N^+ implanted ABCD film is 3500. The AES, XPS and ISS data obtained from these samples indicate that the composition as a function of depth and chemical-state distribution of the species present are similar, which is not the case for 100 and 700°C annealed ABCD films that are not implanted. This implies that the energetic implantation process compensates for low-temperature annealing even though the sample temperature is maintained below 250°C during implantation.

CHAPTER 1
INTRODUCTION

Overview

Ion scattering spectroscopy (ISS), Auger electron spectroscopy (AES), and X-ray photoelectron spectroscopy (XPS) are among the various techniques that were used to analyze the near surface composition of the various chromium films presented in this study. Ion scattering spectroscopy is a highly surface sensitive technique which typically yields compositional and structural information about the outermost atomic layer only. It is performed by impinging a flux of monochromatic inert gas ions such as Ar onto the sample solid surface under vacuum. Compositional information is obtained by analyzing the energies of the ions that scatter off the surface at some preselected angle.

X-ray photoelectron spectroscopy, also known as electron spectroscopy for chemical analysis (ESCA), is a photoemission technique which is widely used to examine the composition and chemical state distribution of species at a solid surface. It is performed by irradiating the solid surface with X-rays under vacuum and measuring the kinetic energy distribution of the emitted electrons. An electrostatic charged particle energy analyzer is used to obtain the spectral peaks generated from the kinetic energies of the emitted electrons. The corresponding binding energies specific to each individual element are then calculated from the following equation:

$$E_b = h\upsilon - E_k + \Delta\phi \qquad (1\text{-}1)$$

where E_b is the electron binding energy (BE) in the solid, E_k is the kinetic energy of the emitted electron and $\Delta\phi$ is the work function difference between the sample and the detector material assuming there is no electrical charging at the sample surface (1).

Auger electron spectroscopy, the most widely used surface analytical technique, also provides compositional and chemical state information in the near surface region. It is performed by measuring the kinetic energies of electrons emitted as a result of an impinging ionizing radiation of electrons at the solid surface. This ionizing radiation results in the formation of a core level hole that decays through a many-body process in which a higher energy electron fills the core-level hole causing emission of either a photon or an Auger electron (2).

Unlike ISS, AES and XPS are techniques that probe at deeper depths beneath the surface and thus do not provide compositional information of the outermost atomic layers. Therefore, the combined use of these complimentary techniques allows for a depth-sensitive assessment of the composition of the surface region of these chromium films.

Literature Review

A method was developed by Sargent (3) and Fink (4) during the 1920s for electroplating conventional Cr films using a sulfate catalyst. These Cr films are bright and retain their brightness indefinitely. This is important because it eliminates a polishing step, which is usually more costly than the plating step. The Sargent bath conditions produce a very clean initial surface for plating so excellent adhesion is obtained in nearly all applications. The fact that surface defects in the base metal are filled in during electroplating also results in smooth surfaces. These favorable characteristics immediately led to the adoption of combination Ni-Cr and Cu-Ni-Cr plates in the automotive and appliance industries as decorative coatings. There are several difficulties with conventional Cr layers, but one of the most limiting is that the hardness of these layers decreases as the annealing or operating temperature increases. As a result, utilization is limited to low-

temperature applications (generally less than 50°C). In 1986 Hoshino, Laitinen and Hoflund (5) described a new method for electroplating amorphous bright chromium deposits (referred to as the ABCD method) from chromic acid solutions containing organic species with -CHO or -COOH groups. These films are superior to conventional films in that they have fewer defects, have smoother surfaces, are more resistant to corrosion by HCl solutions and, most importantly, have significantly increased hardness after annealing at elevated temperatures. Specifically, the hardness of ABCD films increases greatly either by annealing at fairly low temperatures for long periods (200°C for 48 hrs) or higher temperatures for shorter periods (600°C for 1/2 hr) thereby opening new application areas for Cr layers. The hardness of Cr coatings can also be increased using nitrogen implantation. Since the hardness behavior of ABCD films is superior to that of conventional Cr films, it is important to understand the hardness behavior in terms of the chemical nature of these films. Therefore, a series of surface characterization and depth profiling studies of ABCD films (6-8), conventional Cr films (9) and nitrogen-implanted conventional and ABCD films (10-14) have been carried out. Chapters 2 and 3 of this thesis are continuation studies to this series. Chapter 4 details the experimental procedures used to prepare ABCD films using propionic acid as an organic additive which will be characterized in future studies.

CHAPTER 2
SEM/AES STUDY OF CONVENTIONAL AND AMORPHOUS BRIGHT CHROMIUM DEPOSITS

Chromium layers are quite complex compositionally and structurally and change significantly with sample treatment. Nevertheless, the hardness behavior seems to depend primarily upon annealing temperature. These facts suggest that the types of chemical species present and microstructural properties of ABCD films are important in determining their hardness behavior. In this study scanning electron microscopy (SEM), AES coupled with Ar-ion sputtering and scanning Auger microscopy (SAM) have been used to examine conventional Cr platings produced in a Sargent bath (3) and Cr films produced by the amorphous bright chromium deposition (ABCD) method (5) before and after annealing at 700°C for 1 hour in a mechanically pumped 10^{-5} Torr vacuum.

Experimental

Conventional Cr films have been prepared using the standard Sargent bath conditions (3,4), and ABCD layers have been prepared as described previously (5). Both types of films were plated (20 microns thick) onto mild steel substrates and rinsed with distilled water after plating. Some of the samples were annealed at 700°C in a mechanically pumped 10^{-5} Torr vacuum before surface characterization. The experiments were carried out using a JEOL, SEM/SAM system operating at a pressure of 10^{-10} Torr.

Results and Discussion

Conventional Cr Layers

Figure 2-1a shows and electron micrograph (x300) obtained from an as-prepared conventional film. The film appears to be quite rough with many crack defects. A SAM C

map taken from the region on the surface corresponding to that of Figure 2-1a is shown in figure 2-1b. The darker regions are C depleted. This C map indicates that the as-plated surface is fairly uniformly covered with C but that the crack regions have very high C concentrations.

Ion sputtering removes the oxide layer and much of the C. The SEM micrograph shown in figure 1c was taken after sputtering long enough to remove most of the oxide overlayer. The presence of light regions near the grain boundaries suggests that the composition across this sputtered surface is nonuniform. This assertion is verified by the Auger spectra shown in figure 2-2a and b taken from a lighter region near a grain boundary and a darker gray region respectively. The region near the grain boundary contains more C and less O. Thus, both before and after sputtering, the regions near grain boundaries of as-plated conventional Cr layers are C rich.

Significant changes occur in the morphology of the surfaces of these conventional Cr layers with annealing at 700°C for 1 hour in a 10^{-5} Torr vacuum (mechanically pumped) as shown in the electron micrograph (x300) of figure 2-3a. The surface becomes very striated during annealing, and the crack defects are still present. Auger spectra taken using a defocused beam before and after sputtering are shown in figure 2-4a and b respectively. A very large amount of C accumulates on the Cr surface during annealing. This is probably due both to migration of C to the surface from the subsurface region (9) and adsorption of background hydrocarbons on the surface. The shape of the C peak is that of adsorbed hydrocarbons, and its sized compared to the Cr and O peaks indicates that the C overlayer is fairly thick (10~15Å). Furthermore, significant changes have occurred in the spatial distribution of the C as shown in the scanning Auger micrograph in figure 2-3b. After the annealing process the grain boundaries are C depleted compared to the surfaces of the grains. One possibility which would explain this observation is that the C migrates to the surface by grain boundary segregation and then spreads across the surface leaving the grain boundaries C depleted compared to the planar surface regions. Another possibility is

that the hydrocarbons in the background gas preferentially adsorb at the planar surface regions, or that C present at the grain boundaries migrates into the bulk during annealing as observed previously (9). An Auger spectrum taken after sputtering into the bulk of the film is shown in figure 2-4b. The C peak height is quite small as expected. Due to the sizes of the C peak and the signal-to-noise ratio, it is difficult to make any statements about the chemical state of the C based on its Auger peak shape. However, a previous study has shown that the C remaining in the bulk of a conventional Cr film after annealing at 700°C is primarily carbidic (9). A S peak is present which is due to sulfate contained in the electrodeposition bath as a catalyst as well as a peak due to imbedded Ar from the Ar-ion sputtering process. A small amount of O is present throughout these conventional films, and its distribution depends upon the treatment history of the film.

ABCD Layers

A scanning electron micrograph (x300) taken from an as-prepared ABCD film is shown in figure 2-5a. The film surface is much smoother and more defect free that the as-prepared conventional layer. A large crack (not a grain boundary) appears in this micrograph. This crack may be due to the fact that these Cr layers were deposited on foils which may have been bent during handling causing the Cr films to crack. Most of the surface is quite smooth and uniform without cracks.

An Auger spectrum taken from the as-plated ABCD layer is shown in figure 2-6a. This surface contains more O, S and K than the as-plated conventional Cr layers and less C. The C scanning Auger micrograph shown in figure 2-5b indicates that the C is uniformly distributed across the surface of the ABCD layer, and the C peak shape in figure 2-6a suggests that the surface C is in the form of adsorbed hydrocarbons. An Auger spectrum taken after sputtering into the bulk ABCD layer is shown in figure 2-6b. Peaks due to S, K and O are not present, but a peak due to embedded Ar does appear. Most importantly a large C peak remains, but the shape of this C peak is changed to that of

carbidic. Based on a SiO_2 standard, the sputtering conditions used yield a sputter rate of about 140Å/min. The ABCD sample was sputtered 50 s between taking the Auger spectra shown in figure 2-6a and b. The Auger spectra taken during sputtering show that the C peak shape changes from hydrocarbon like to carbidic very rapidly (after removing less than 20Å of the surface layer). This behavior is very different from that of as-plated conventional Cr layers and must be due to the fact that specific C compounds containing -CHO or -COOH groups are introduced into the electrochemical bath and that different bath operating conditions used to prepare ABCD films. Ion sputtering converts the C-containing species into carbides much like annealing.

An electron micrograph (x300) taken from an ABCD film annealed at 700°C for 1 hour in a mechanically pumped 10^{-5} Torr vacuum is shown in figure 2-7a. Unlike the conventional Cr layer, the surface of the ABCD film is changed very little during the annealing step except for the appearance of some very small striations. A corresponding Auger spectrum taken from the annealed ABCD surface before sputtering is shown in figure 2-8a. Like the annealed, conventional Cr surface, this Auger spectrum from the annealed ABCD film exhibits a large hydrocarbon-like C peak which probably originates mostly from adsorption of background hydrocarbons during the annealing step. The SAM C map shown in figure 2-7b again indicates a uniform C distribution. An Auger spectrum taken from the same annealed ABCD sample after removing about 200Å by ion sputtering is shown in figure 2-8b. The C peak shape is still carbidic after annealing and sputtering, and a significant amount of O is present in the subsurface region.

Summary

An SEM/AES study comparing conventional Cr and ABCD films before and after annealing at 700°C for 1 hour in a mechanically pumped 10^{-5} Torr vacuum has been carried out. The data demonstrates significant differences between the two types of films which apparently are responsible for the superior properties of annealed ABCD films. The

surfaces of as-plated conventional Cr films are very rough and are laden with crack defects. Annealing causes these surfaces to become even rougher through the formation of a striated texture. However, the as-prepared ABCD layers are quite smooth and remain so after annealing.

Interesting differences occur in the C chemical state, amounts and spatial distribution between the conventional and ABCD films before and after annealing. The C at the surfaces of all the Cr layers is hydrocarbon like, but the chemical nature of the C in the ABCD films changes very rapidly with depth as the hydrocarbon layer is ion sputtered away. This C is carbidic in the ABCD layers and is uniformly distributed across the surface.

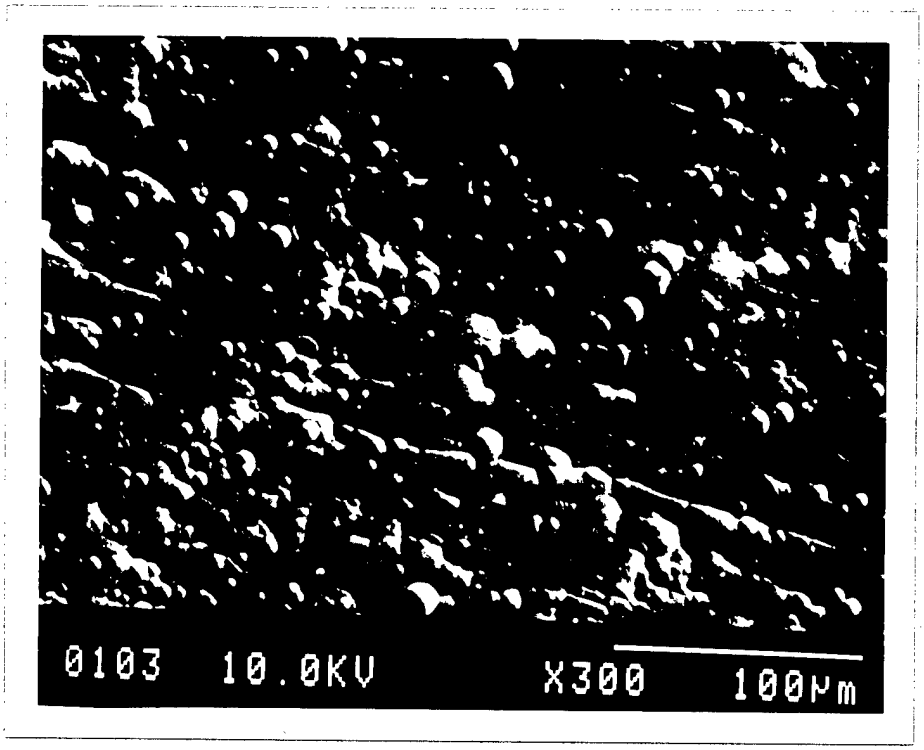

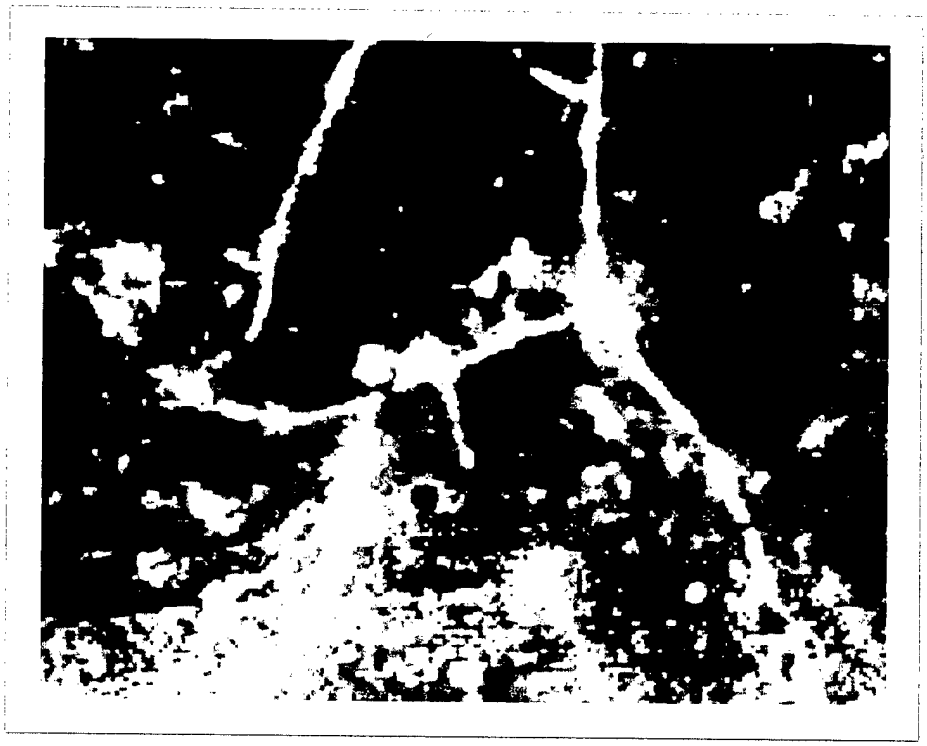

Figure 2-1. (a) Electron micrograph (x300) obtained from an as-plated, conventional Cr layer. (b) scanning Auger C map taken from the same region as the electron micrograph shown in (a). The darker regions contain less C. (c) electron micrograph taken from the same region as (a) and (b) after ion sputtering long enough to remove most of the oxide layer.

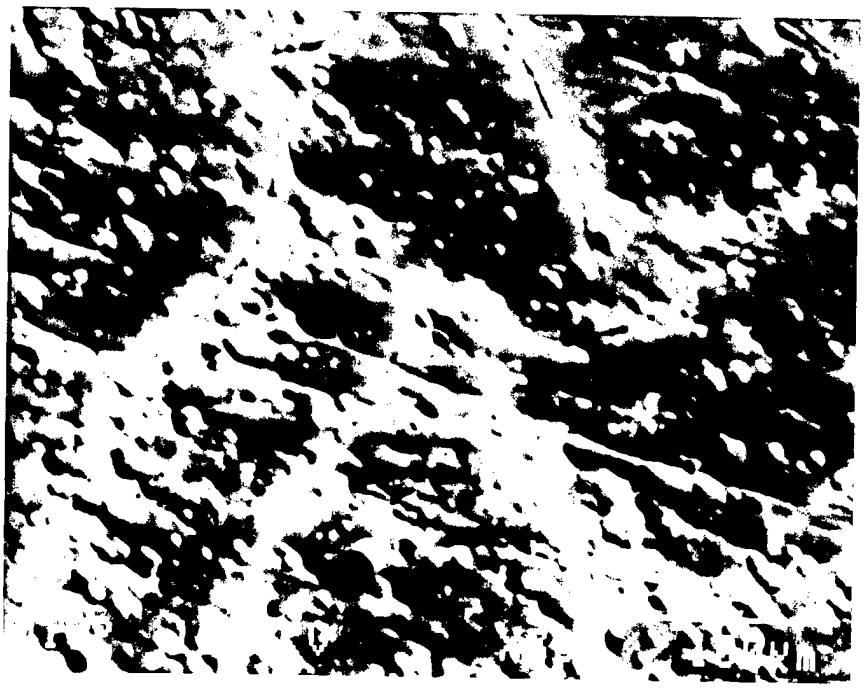

Figure 2-1. continued

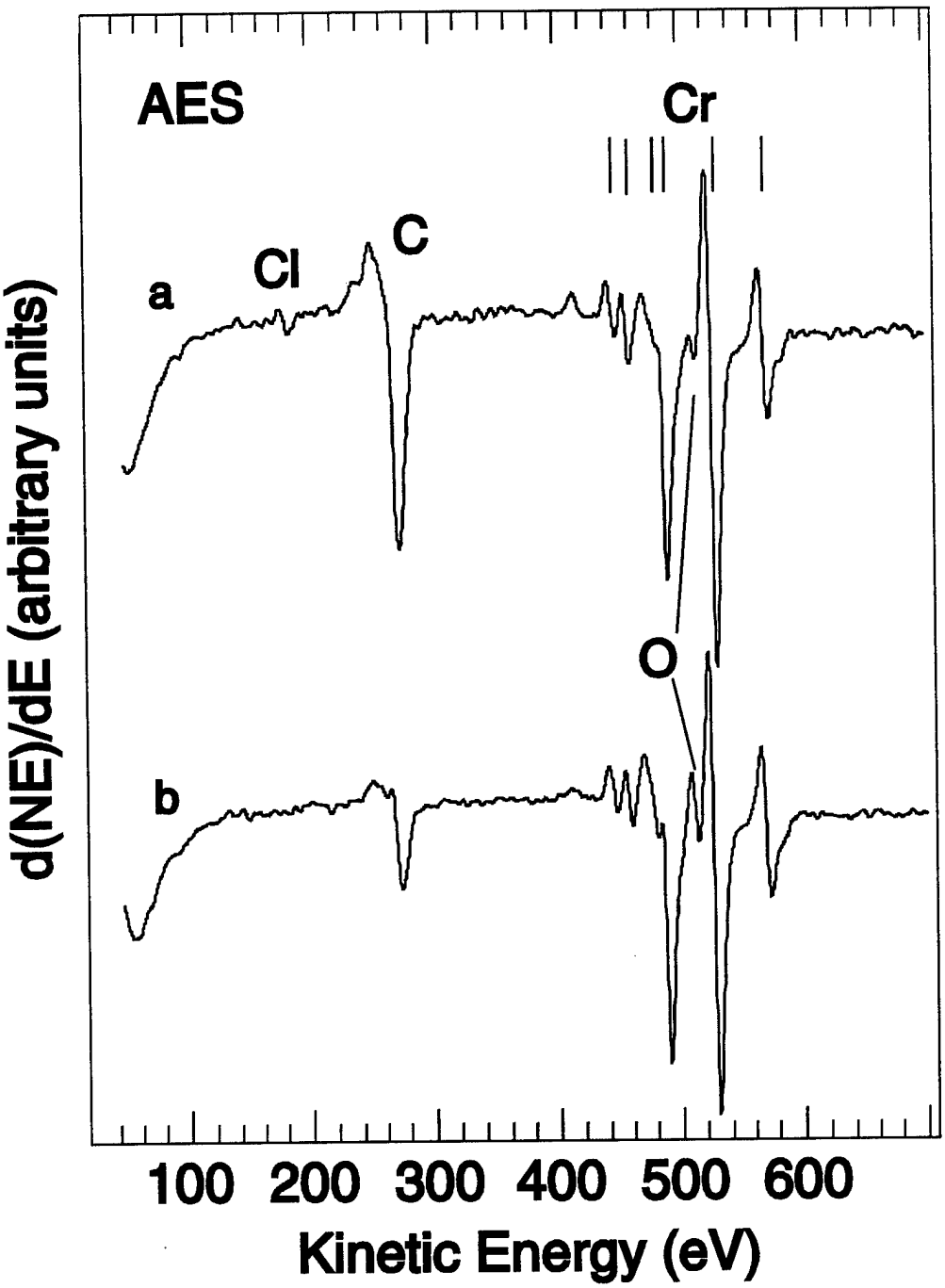

Figure 2-2. Small spot Auger spectra taken from (a) a light gray region near a grain boundary and (b) a darker gray region in the electron micrograph shown in figure 1c.

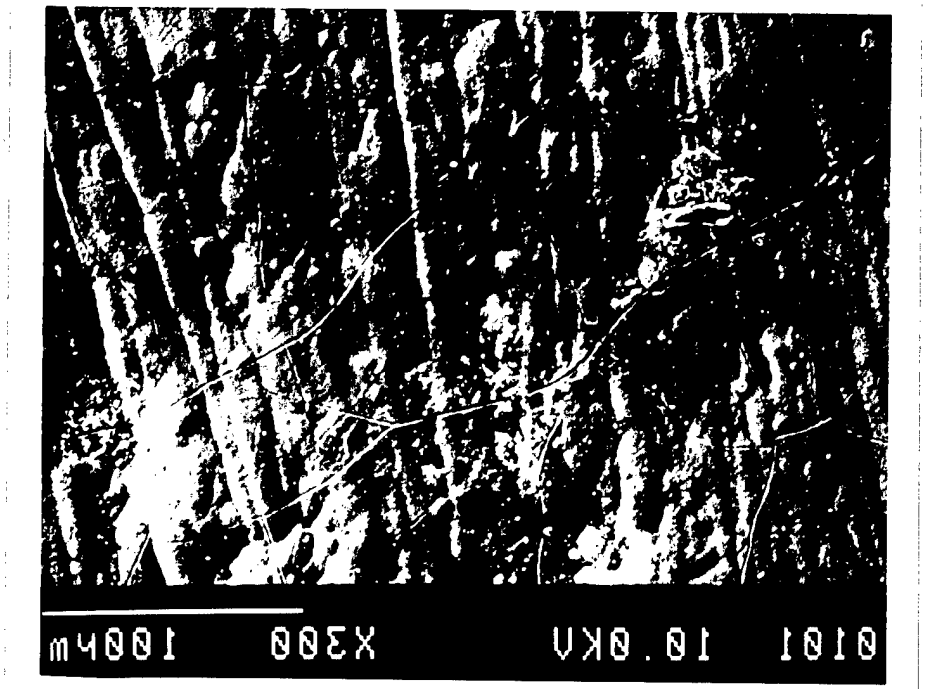

Figure 2-3. (a) Electron micrograph (x300) taken from a conventional Cr layer after annealing at 700°C in a mechanically pumped 10^{-5} Torr vacuum for 1 hour. (b) C Auger map taken from the same region as the electron micrograph shown in (a). The darker regions contain less C.

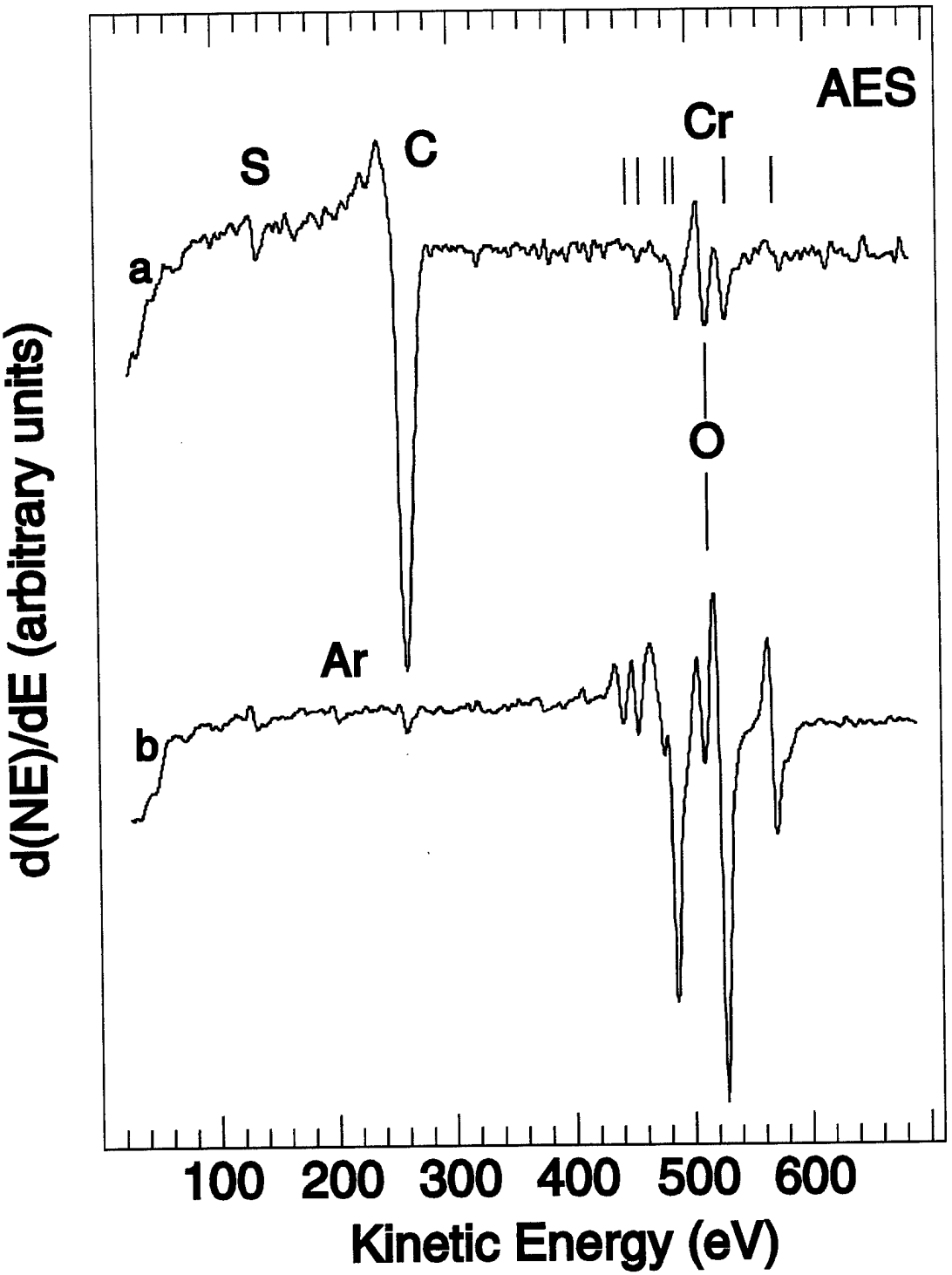

Figure 2-4. Auger spectra taken (a) before and (b) after ion sputtering a conventional Cr film at 700°C in a 10^{-5} Torr vacuum for 1 hour.

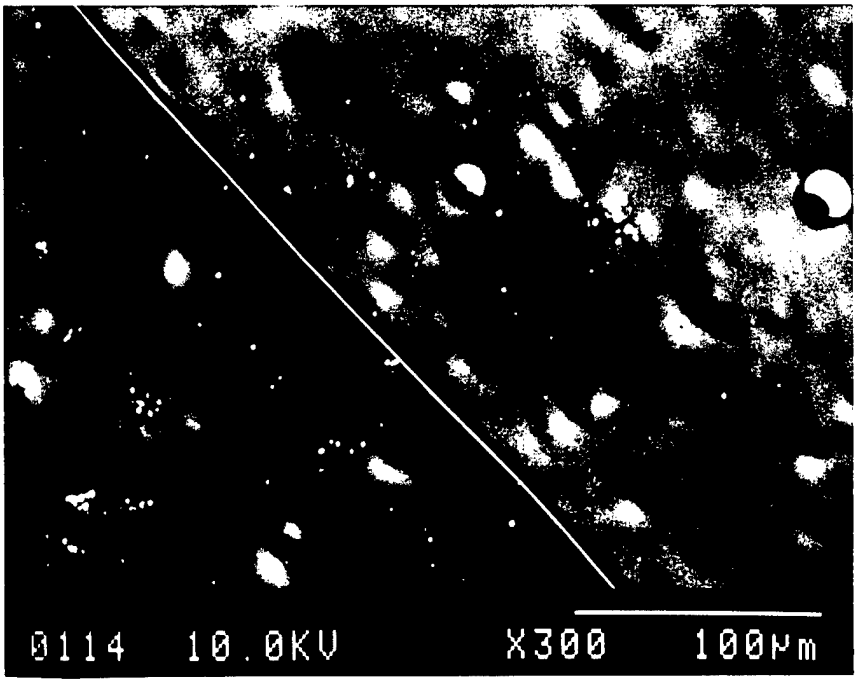

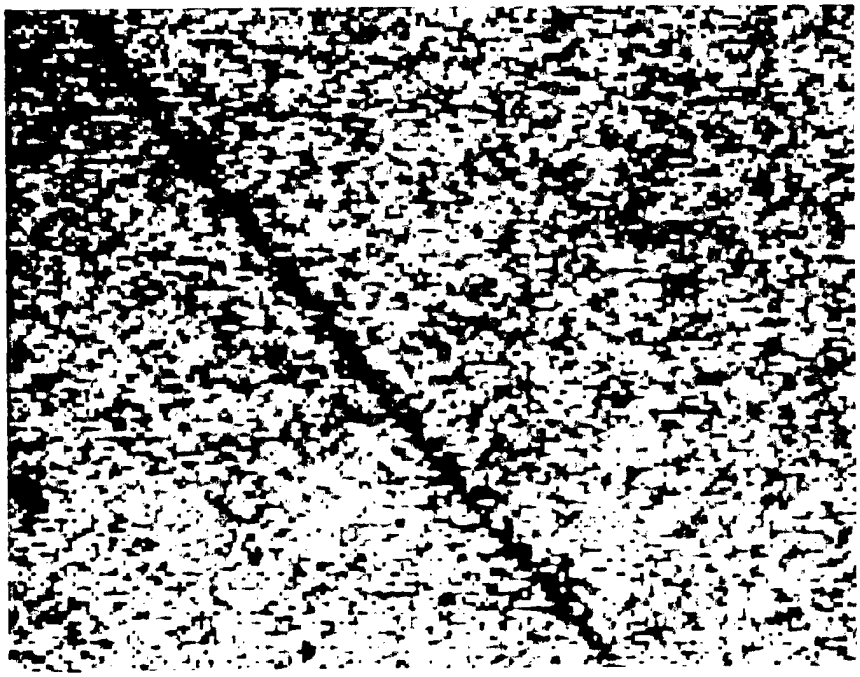

Figure 2-5. (a) Scanning electron micrograph (x300) taken from an as-prepared ABCD film and (b) scanning Auger C micrograph taken from the same region of the sample as (a).

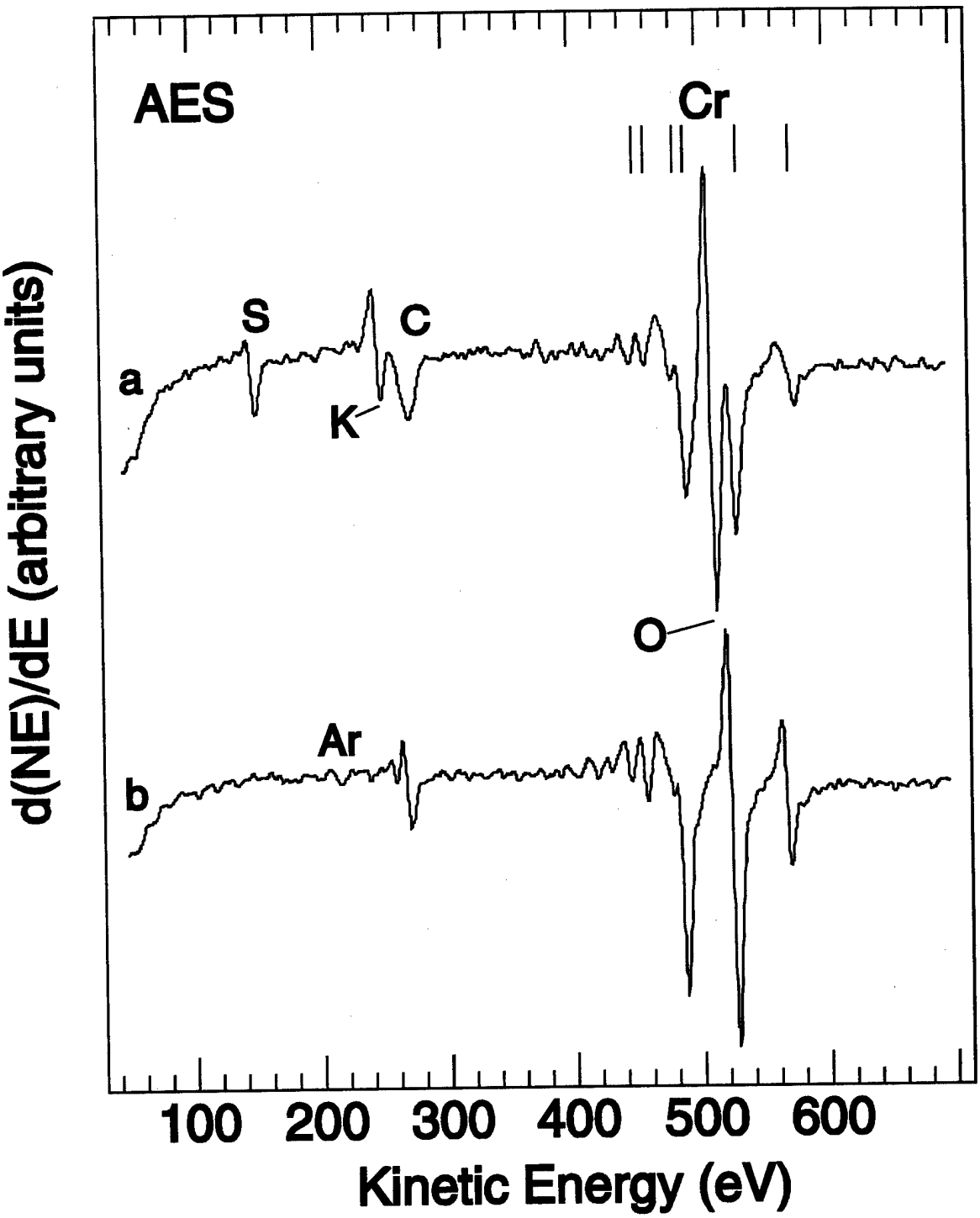

Figure 2-6. Auger spectra taken from (a) an as-plated ABCD layer and (b) the same surface after ion sputtering into the bulk.

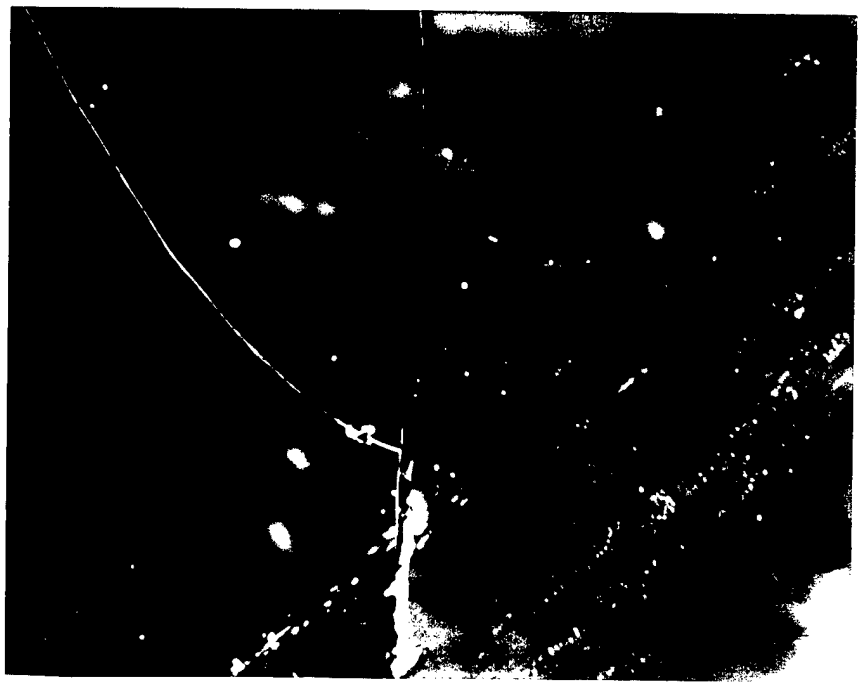

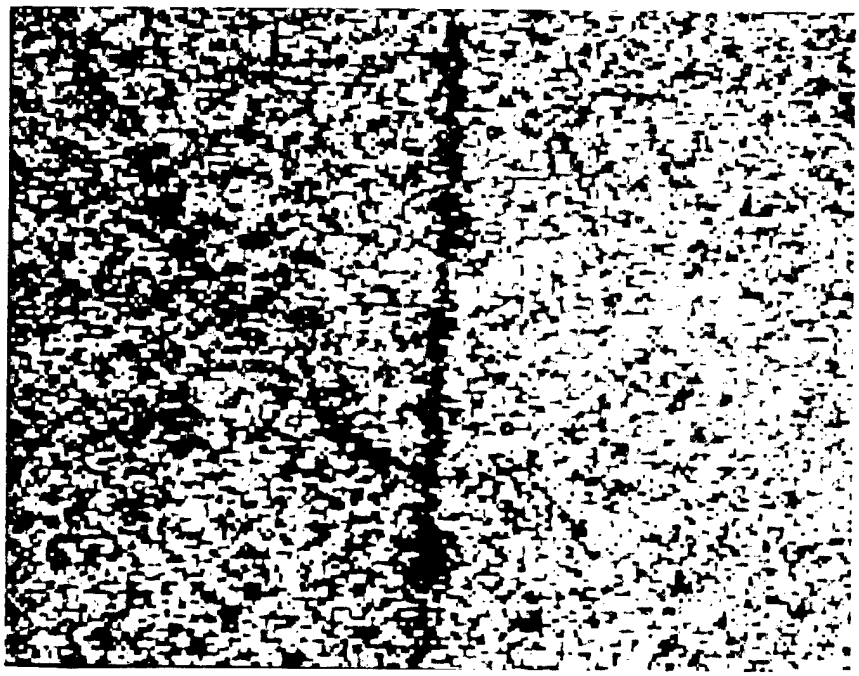

Figure 2-7. (a) Scanning electron micrograph (x300) taken from an ABCD film after annealing at 700°C for 1 hour in a mechanically pumped 10^{-5} Torr vacuum and (b) C scanning Auger micrograph taken from the same region as (a).

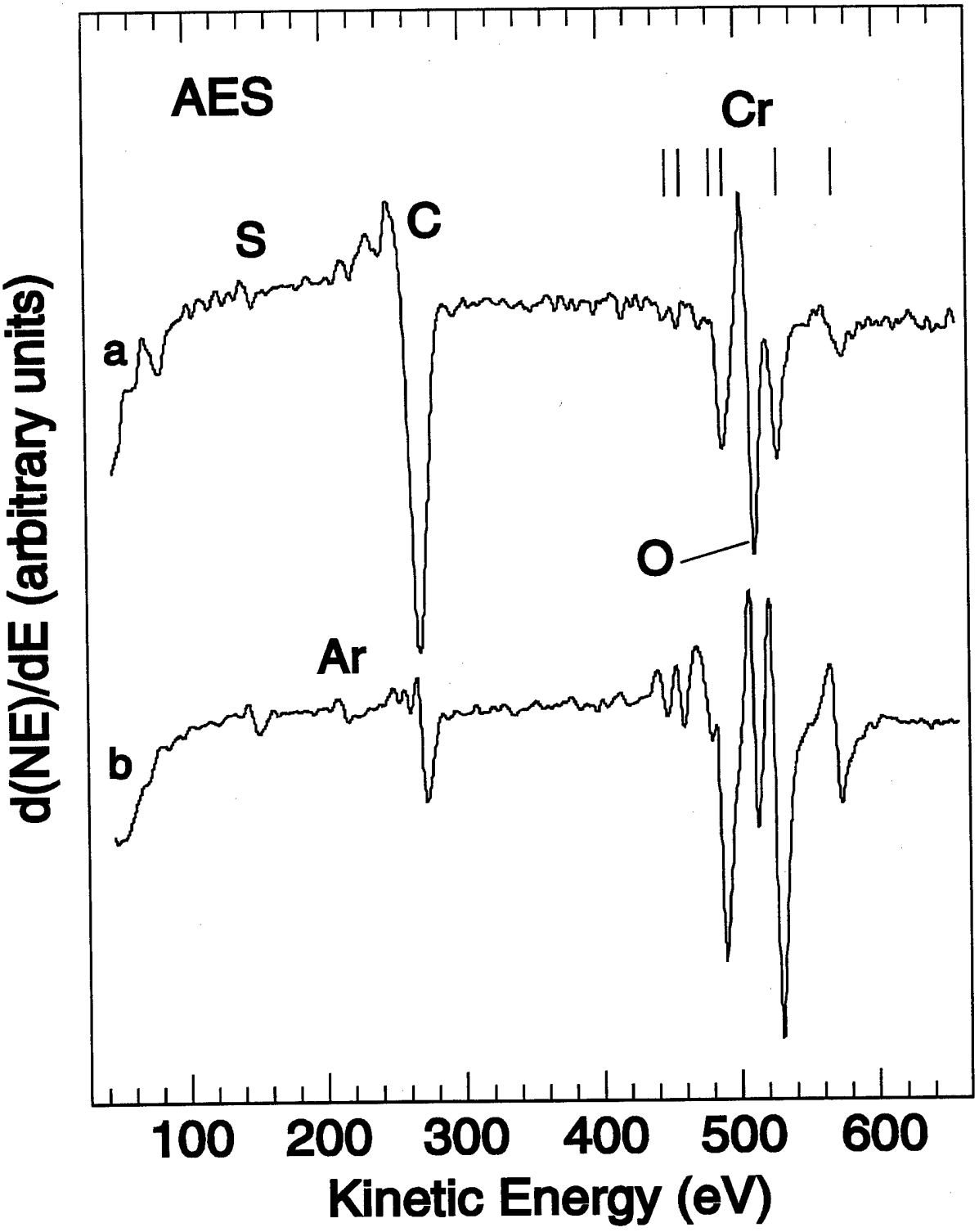

Figure 2-8. Auger spectra taken from an ABCD film (a) before and (b) after annealing at 700°C for 1 hour in a 10^{-5} Torr vacuum.

CHAPTER 3
CHARACTERIZATION STUDY OF N^+-IMPLANTED, AMORPHOUS BRIGHT CHROMIUM DEPOSITED (ABCD) FILMS

Since changing the chemical composition of the plating bath alters the mechanical properties of the Cr films produced, the chemical makeup as well as the microstructural characteristics play an important role in determining film properties. Therefore, the goal of this surface characterization study is to determine the chemical composition and the chemical species present in these films as a function of depth with an ultimate objective of understanding the relationship between chemical makeup, microstructure and mechanical properties which are all dependent upon the annealing and implantation conditions used prior to characterization. In this study 100 and 700°C annealed ABCD films have been N^+ implanted, and the films have been characterized using ISS, XPS and AES coupled with sputter depth profiling. A related study of N^+-implanted conventional Cr layers has been published previously (12).

Experimental

The ABCD films were prepared using conditions described by Hoshino, Laitinen and Hoflund (5) and then annealed at 100 and 700°C in a mechanically pumped 10^{-5} Torr vacuum for 1/2 h. Ion implantation was carried out using 90-keV N^+ to a total dose of 1 x 10^{18} ions/cm^2. The retained N ion dose is 4.0 x 10^{17} and 7.2 x 10^{17} for the ABCD samples annealed at 100 and 700°C respectively. A low flux was used in order to minimize heating of the sample surface region during implantation. Although it was not possible to measure sample temperature during implantation, the sample temperature most likely remained below 250°C. Ion scattering spectroscopy, XPS, AES and sputter-depth profiling were used in the manner described previously (12) to examine the surface and

bulk regions of the two implanted ABCD films. The sputter rate is estimated to be about 0.03 nm per min.

Results and Discussion

The hardness of conventional Cr and ABCD films has been determined after various treatments in previous studies (5,10-12,15), and the results are summarized in table 3-1. Knoop hardness measurements were performed because the load could be varied in order to vary the depth sensitivity of the measurement. Based on the diameter of the imprint formed using the lightest load of 10 mN, the most surface-sensitive hardness measurement samples the outermost 200 nm. This is characteristic of the thickness of the implanted layer (10). A number of facts are apparent from the data in table 3-1: (1) implanting greatly increases the hardness of conventional Cr but only if the sample is not annealed, (2) the outermost surface region is harder than the subsurface region, (3) annealing conventional layers decreases the hardness, (4) annealing and implanting ABCD layers both increase the hardness of these films, and (5) ABCD films which are annealed at elevated temperatures and implanted yield the highest hardness values. The 100- and 700°C annealed and N^+ implanted ABCD films examined in this study have surface-sensitive Knoop hardnesses of 3280 and 3500 respectively, which are quite similar even though the annealing temperatures are quite different. The 100°C annealed ABCD film which was not implanted has a hardness of only 1500 so N^+-implanting has a large influence in this case. In comparison N^+-implanting the 700°C annealed sample has a much smaller effect (3360 $\rightarrow$ 3500).

An Auger spectrum obtained from the ABCD sample after annealing at 100°C and N^+ implanting is shown in figure 3-1a. The predominant peaks are due to chromium, oxygen, nitrogen, carbon and sulfur. The carbon peak is relatively large and its shape is characteristic of adsorbed hydrocarbons. Similar carbon peaks are typically found on these Cr surfaces. The chromium and oxygen peaks are smaller in comparison and are

characteristic of Cr oxides and hydroxides. Nitrogen and sulfur are present in smaller but significant amounts in the near-surface region of the film. The nitrogen is mostly due to N^+ implantation, but a small amount may also be attributed to nitrate impurities in the electroplating bath. Sulfur is used as a catalyst in the plating operation and is deposited in small quantities throughout the film.

The Auger spectrum shown in figure 3-1b was obtained from the 100°C annealed and N^+ implanted film after sputtering for 105 min using 1-keV Ar^+ ions. For the sputtering conditions used, this corresponds to a depth of approximately 30 Å beneath the surface. As a result of sputtering, much of the hydrocarbon and surface oxide layer is removed yielding a lower oxygen-to-chromium ratio. The carbon peak is smaller, and its shape is more characteristic of a carbide. This is discussed in more detail below in conjunction with the XPS C 1s spectra. The nitrogen peak is larger as expected, and the surface S is removed by sputtering. Also, a peak due to implanted Ar is apparent. The spectrum shown in figure 3-1c was taken after sputtering the same film for 135 min (~ 40 Å). The carbon peak is smaller and its shape is changed although it still remains carbidic in nature. The concentrations of Cr, N and O are increased in this region of the film.

An Auger spectrum obtained from the ABCD sample preannealed at 700°C and N^+ implanted is shown in figure 3-2a, and spectra obtained after Ar^+ sputtering for 75 min and 150 min are shown in figure 3-2b and c respectively. The carbon concentration throughout this film is smaller than in the 100°C annealed and N^+ implanted sample, but the carbon Auger peak shapes follow the same trend. The spectrum shown in figure 3-2a exhibits a larger oxygen-to-chromium peak height ratio indicating that this surface is more fully oxidized than that of the 100°C annealed and N^+ implanted film. Again the N peak height increases with sputtering. The near-surface region of this sample has a larger sulfur concentration due to migration of sulfur to the surface during the high-temperature anneal.

The Auger composition profile data for the samples annealed at 100 and 700°C and N^+ implanted are shown in figures 3-3 and 3-4 respectively. The compositional

information was calculated using published sensitivity factors (2), the homogeneous assumption and peak-to-peak heights obtained from Auger spectra taken intermittently during sputtering. The profiles in figures 3-3 and 3-4 are semiquantitative because preferential sputtering (6), matrix effects and peak-shape changes due to alteration of chemical states (9) were not considered in the data analysis.

The Auger compositional profiles in figure 3-3 obtained from the 100°C annealed and N^+ implanted film exhibit three distinct layers with different compositions. The outermost layer is approximately 5 Å thick and is sputtered away in about 18 min. The surface composition contains about 58 at% C, 20 at% Cr, 12 at% O, 8 at% N, and 2 at% S indicating that this layer consists primarily of hydrocarbon contamination. From 5 to 32 Å (18 to 108 min of sputtering) below the surface, the composition remains relatively constant and consists of about 37 to 42 at% C, 35 at% Cr, 17 to 23 at% N, and 5 at% O. Below 32 Å there is a sharp increase in the Cr and O concentrations to about 41 at% and 13 at% respectively and a corresponding decrease in C to 22 at%. The N concentration rises steadily to 25 at%.

The Auger compositional profiles obtained from the 700°C annealed and N^+ implanted film exhibit a greater variation in concentrations with sputter time as shown in figure 3-4. The outer layer, which is about 5 Å thick, is sputtered away in 18 min and has a composition of about 31 at% C, 20 at% Cr, 22 at% O, 21 at% S, and 6 at% N. With sputtering the Cr concentration rises rapidly to 38 at% and levels out to 41 at% between 14 and 40 Å (45 to 120 min of sputtering), dropping slightly to 37 at% at 45 Å (150 min of sputtering). The C content remains nearly constant at 28 at% between 5 and 40 Å after which it drops sharply to 19.5 at% at 150 min. The N profile rises steadily throughout the film from 17 at% after removal of the outer layer to 25 at% at 45 Å. After 18 min the O concentration drops from 14 to 9 at% at 14 Å and remains relatively constant at about 40 Å (120 min of sputtering) after which it increases to about 15 at% at 150 min. The S concentration is low throughout the bulk of the film ranging from 4 at% after 18 min of

sputtering and drops to 1 at% at 120 min of sputtering before rising again to 3.5 at% after 150 min of sputtering.

Ion scattering spectroscopy spectra obtained from the sample annealed at 100°C and N^+ implanted before sputtering, after sputtering for 15 min, and after sputtering for 135 min are shown in figure 3-5a, b and c respectively. The spectrum shown in a contains a large feature in the low E/E_0 range due to C, N and O. The shape of this feature is characteristic of those obtained from surfaces of as-prepared samples, which are covered by an adsorbed film of hydrocarbons (12). A small Cr peak is apparent at an E/E_0 of 0.72. The hydrocarbon layers are usually thicker on similarly treated as-prepared conventional films so they do not yield this Cr peak (12). The spectra shown in figures 3-5b and c contain predominant O and Cr peaks with shoulders on the O peak due to C and N, and the largest peak in both spectra is the Cr peak. The very small peak at an E/E_0 of 0.87 is probably a multiple scattering peak (9). Both C and N are lighter in mass so they have smaller ISS cross sections. Furthermore, they may be preferentially sputtered away more rapidly than the O in the outermost atomic layer where the sputter damage is greatest so the data shown in figure 3-5 is not as quantitative as the Auger data. The O-to-Cr peak height ratio is larger in spectrum c than spectrum b which is consistent with the Auger compositional data shown in figure 3-3. The ISS spectra obtained before and after 150 min of sputtering are shown in figure 3-6a and b respectively. These spectra are quite similar to those obtained from the 100°C-annealed and N^+ implanted sample.

The XPS survey spectra obtained from the 100°C-annealed and N^+ implanted sample before and after sputtering for 135 min are shown in figure 3-7a and b respectively. The spectrum taken before sputtering contains a predominant C 1s peak, O 1s and Cr 2p peaks of similar size and a small N peak. After sputtering the C 1s and O 1s peaks are reduced with respect to the Cr 2p feature, and the N peak height is increased, which is consistent with the Auger compositional profile data shown in figure 3-3. The S peaks are not observed in the XPS survey spectra due to its low sensitivity factor. Similar trends are

found in the XPS survey spectra obtained from the 700°C-annealed and N^+ implanted sample before and after 150 min of sputtering as shown in figure 3-8a and b respectively, but there are several differences. Consistent with the AES data, the O-to-Cr ratio for the as-prepared sample annealed at 700°C and N^+ implanted is almost twice that of the sample annealed at 100°C and N^+ implanted indicating that the near-surface region of the 700°C-annealed and N^+ implanted sample is more fully oxidized than the 100°C-annealed and N^+ implanted sample. After sputtering, the O-to-Cr ratio is reduced and appears to be quite similar to that obtained from the sample annealed at 100°C and N^+ implanted after sputtering (figure 3-7b), which is also consistent with the Auger data shown in figures 3-3 and 3-4.

High-resolution XPS Cr 2p spectra obtained from the 100°C-annealed and N^+ implanted sample before and after 135 min of sputtering and from the 700°C annealed and N^+ implanted sample before and after 150 min of sputtering are shown in figure 3-9a, b, c and d respectively. Similar trends in peak shapes and sizes are exhibited by both samples before and after sputtering. In figure 3-9a several shoulders are apparent on the high-BE side of the Cr $2p_{3/2}$ peak that may be attributed to Cr_2S_3, CrN, Cr_2N, various chromium oxides such as CrO_2, Cr_2O_3, CrO_3, and CrCOOH. Examination of the Cr $2p_{1/2}$ peak in figure 3-9a reveals two peaks of approximately equal size centered at 583.6 eV and 585.5 eV. One of these peaks is 9.2 eV higher than the Cr $2p_{3/2}$ peak and corresponds to metallic Cr (15). The other Cr $2p_{1/2}$ peak is indicative of other Cr states such as CrN and Cr_2N as well as various chromium oxides. The corresponding spectrum obtained from the sample annealed at 700°C and N^+ implanted (figure 3-9c) indicates that the near-surface region of this sample is more fully oxidized than that of the 100°C-annealed and N^+ implanted sample. The Cr $2p_{1/2}$ feature shown in figure 3-9c is broader, centered around 585.5 eV, lacks the double-peak structure and contains a larger contribution from oxides than the peaks in figure 3-9a. After sputtering both samples exhibit Cr $2p_{3/2}$ peaks that are predominantly metallic Cr in nature with shoulders on the high-BE side attributable to Cr

oxides and Cr nitrides. A Cr $2p_{1/2}$ feature which is 9.2 eV higher than the Cr $2p_{3/2}$ peak is observed in both cases and is characteristic of metallic Cr. In figure 3-9d the oxide and nitride shoulders are larger than those in figure 3-9b which again is consistent with the Auger data discussed above. The Cr 2p BEs for chromium carbides including Cr_2C_3, Cr_3C_7 and Cr_6C_{23} have not been published so no attempt is made to assign these species in figure 3-9 even though they are present in quite significant quantities.

High-resolution XPS O 1s spectra obtained from the 100°C annealed and N^+ implanted sample before and after sputtering for 135 min and from the 700°C-annealed and N^+ implanted sample before and after sputtering for 150 min are shown in figure 3-10a, b, c and d respectively. A peak centered at 530.2 eV corresponding to CrO_3 is predominant in figure 3-10a. The asymmetry of the peak indicates the presence of Cr_2O_3, $Cr(OH)_3$ and CrO_2. A small amount of adsorbed H_2O is also present. Sputtering removes the adsorbed H_2O feature, reduces the size of the O 1s feature and changes its shape (figure 3-10b). The primary contributions to this feature are from CrO_3 and CrO_2. Two distinct shoulders are present on the high-BE side due to Cr_2O_3 and $Cr(OH)_3$. The spectrum shown in figure 3-10c is similar in shape to that in 3-10a, but it is larger as expected and the contributions due to $Cr(OH)_3$ and Cr_2O_3 are larger. The size of this peak is reduced by sputtering, but it is still larger than the O 1s feature in figure 3-10b. This is consistent with the Cr 2p spectra in figure 3-9 and the Auger data discussed above. Sputtering the sample annealed at 700°C and N^+ implanted results in changes similar to those for the 100°C-annealed and N^+ implanted sample except that the O 1s feature obtained from the 700°C-annealed and N^+ implanted sample is larger and contains a larger contribution from CrO_2.

The XPS C 1s spectra obtained from the sample annealed at 100°C and N^+ implanted before and after sputtering for 135 min and obtained from the sample annealed at 700°C and N^+ implanted before and after sputtering for 150 min are shown in figure 3-11a, b, c and d respectively. The spectra obtained from both samples before sputtering (figures 3-11a and c) exhibit a single large symmetrical peak centered at 284.7 eV due to adsorbed

hydrocarbons. However, these features exhibit structure on the low-BE side due to the presence of subsurface carbides. These carbides become quite prominent after sputtering as shown in figure 3-11b and d respectively. Based on the relative peak sizes of the hydrocarbon and carbide peaks in these spectra, the hydrocarbon layer is thicker on the 700°C annealed and N^+ implanted sample. This is consistent with the Auger data also. The presence of these carbides and their microstructural distribution are responsible for the extreme hardness of these films (5). Chromium carbides also form during the N^+ implantation of conventional layers in significant amounts near the surface which contributes to their high hardness values (12).

High-resolution XPS N 1s spectra obtained from the 100°C-annealed and N^+ implanted sample before and after sputtering for 135 min and obtained from the 700°C-annealed and N^+ implanted sample before and after sputtering for 150 min are shown in figure3-12a, b, c and d respectively. Binding energy assignment lines for CrN, Cr_2N and molecular nitrogen are shown at 396.7 397.4 and 399.8 eV respectively. The CrN is the predominant species in all four spectra with small contributions from Cr_2N in both as-prepared samples. A small peak due to molecular nitrogen is also present in all four spectra. As the implanted N dose is increased, more N_2 is formed as inclusions or bubbles within the Cr film. The fact that the N species present in these layers do not appear to change much with sputtering or annealing temperature indicates that the N species formed during implantation does not depend upon the chemical composition of the film being implanted. This assertion is supported by the fact that conventional films annealed at 700°C also form CrN almost exclusively and exhibit similar small N_2 peaks (12).

Generally, these annealed and N^+ implanted ABCD films exhibit similar chemical state characteristics as conventional, annealed and N^+-implanted Cr films studied previously (12). Both consist of an outermost carbon-rich layer primarily due to adsorbed hydrocarbons. Chromium is present primarily in the form of oxides near the outermost surfaces of both types of films. After sputtering the O-to-Cr ratios are reduced in both

types of films and chromium is present predominantly in metallic and nitride form. In both cases implantation tends to favor the formation of CrN, but small amounts of molecular nitrogen are also present. Conventional films however, contain significantly less amounts of carbides in the implanted regions than ABCD films. The higher concentration of carbides present throughout the bulk of ABCD films is responsible for its superior hardness values over conventional films as shown in table 3-1.

Summary

X-ray photoelectron spectroscopy, ISS and AES coupled with sputter depth profiling have been used to examine the chemistry of N^+-implanted ABCD films preannealed at 100 and 700°C. Both pre-sputtered samples contain a surface layer of adsorbed hydrocarbons and a small amount of water. Oxygen is also present in the form of Cr oxides, predominantly CrO_3 and Cr_2O_3, with the 700°C annealed and N^+-implanted sample being more fully oxidized than the 100°C annealed and N^+ implanted sample. Sputtering removes most of the hydrocarbons and water and reduces the oxygen-to-chromium ratio from 1.6 to 0.4 for the 100°C-annealed and N^+ implanted sample and from 2.5 to 0.5 for the 700°C-annealed and N^+ implanted sample. The chemical state of the chromium changes from oxidic at the surface to primarily metallic and CrN and Cr carbides beneath the surface. The remaining oxide species after sputtering are predominantly CrO_3 and CrO_2. The presence of the carbides and their microstructural distribution are responsible for the extremely high hardness values of these films. The N^+ implantation favors the formation of CrN regardless of annealing temperature or chemical composition of the film being implanted. Small amounts of molecular nitrogen are also observed throughout both films. The combination of Cr nitride in conjunction with the Cr carbides yield considerable improvements in hardness compared to similarly annealed ABCD films that have not been implanted, and the carbide concentrations in N^+-implanted ABCD films

are higher than those in N^+-implanted conventional films, which is responsible for the increased hardness of N^+-implanted ABCD films.

Table 3-1. Knoop Hardness for Conventional and ABCD Layers after Various Treatments

Cr Sample (Annealing Temperature	10 mN Load	25 mN Load	50 mN Load
Conventional, non-implanted (600°C)	650	540	460
Conventional, implanted (600°C)	825	530	470
Conventional, non-implanted (non-annealed)	1030	870	800
Conventional, implanted (non-annealed)	---	---	2250
ABCD, non-implanted (100°C)	1500	1250	1050
ABCD, implanted (100°C)	3280	2250	1910
ABCD, non-implanted (700°C)	3360	2480	2280
ABCD, implanted (700°C)	3500	2400	2300

Table 3-2. XPS Binding-Energy Assignments

Assignment Line	Species	Binding Energy
O 1s	Cr_2O_3	531.0
O 1s	$Cr(OH)_3$	531.7
O 1s	$Cr(CO)_6$	534.3
O 1s	adsorbed H_2O	533.2
O 1s	hydroxyl groups	533.0
O 1s	CrO_3	530.2
O 1s	CrO_2	529.3
Cr $2p_{3/2}$	metal	574.3
Cr $2p_{3/2}$	Cr_2S_3	574.8
Cr $2p_{3/2}$	CrN	575.8
Cr $2p_{3/2}$	CrO_2	576.3
Cr $2p_{3/2}$	Cr_2N	576.1
Cr $2p_{3/2}$	Cr_2O_3	576.8
Cr $2p_{3/2}$	CrOOH	577.0
Cr $2p_{3/2}$	$CrCl_3$	577.4
Cr $2p_{3/2}$	CrO_3	578.3
C 1s	Cr_3C_2	282.8
C 1s	Cr_7C_3	282.9
C 1s	C (graphitic)	284.5
C 1s	Cr(acac)3	285.95
N 1s	CrN	396.7
N 1s	Cr_2N	397.4
N 1s	N_2	399.8

Table 3-3. XPS O/Cr Peak Area Ratios

Annealing Temperature (°C)	Sputter Time (min)	O/Cr
100	0	1.6
100	135	0.4
700	0	2.5
700	150	0.5

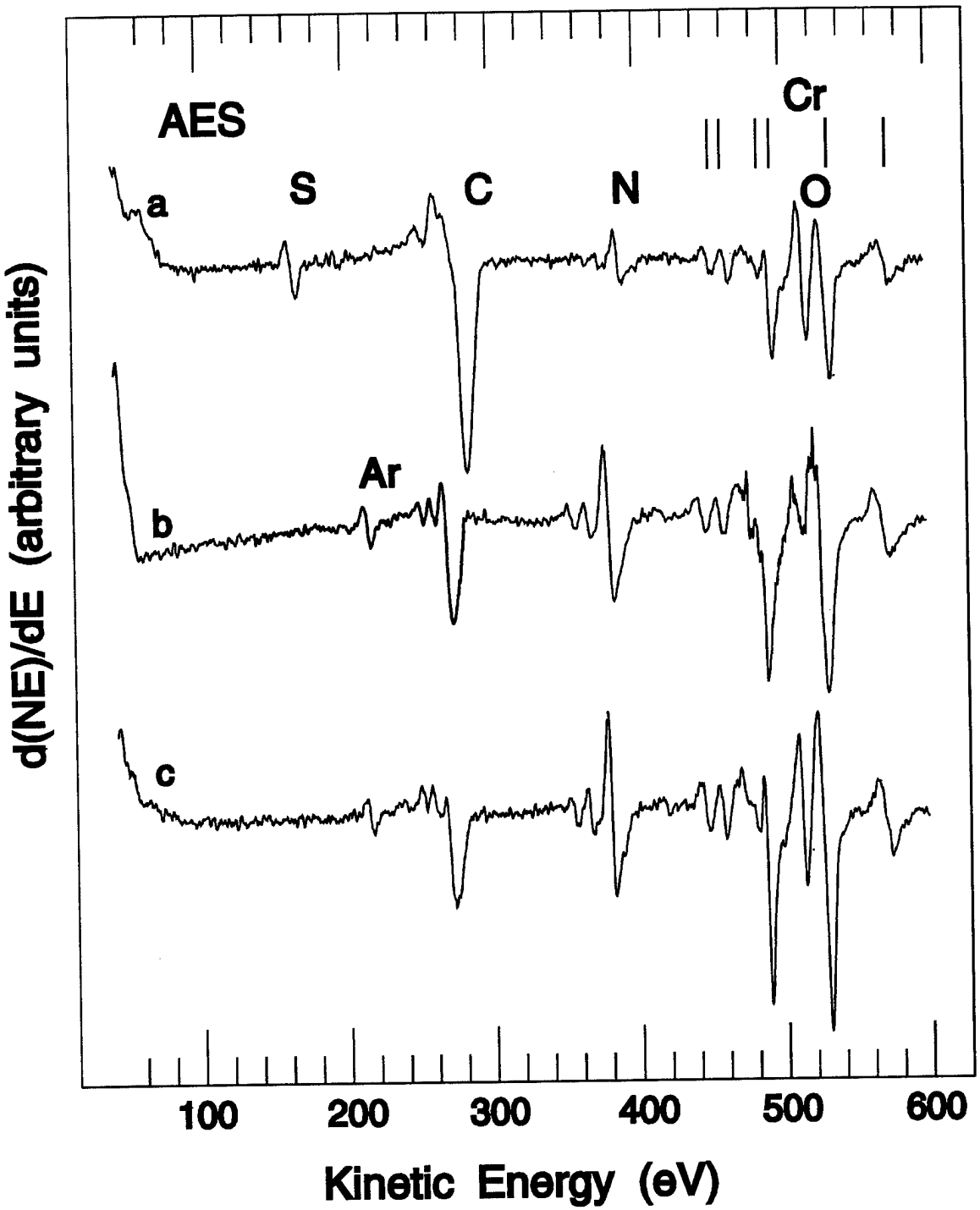

Figure 3-1. Auger spectra taken (a) from an ABCD Cr sample annealed at 100°C and N^+ implanted, (b) after Ar^+ sputtering for 105 min and (c) after Ar^+ sputtering for 135 min.

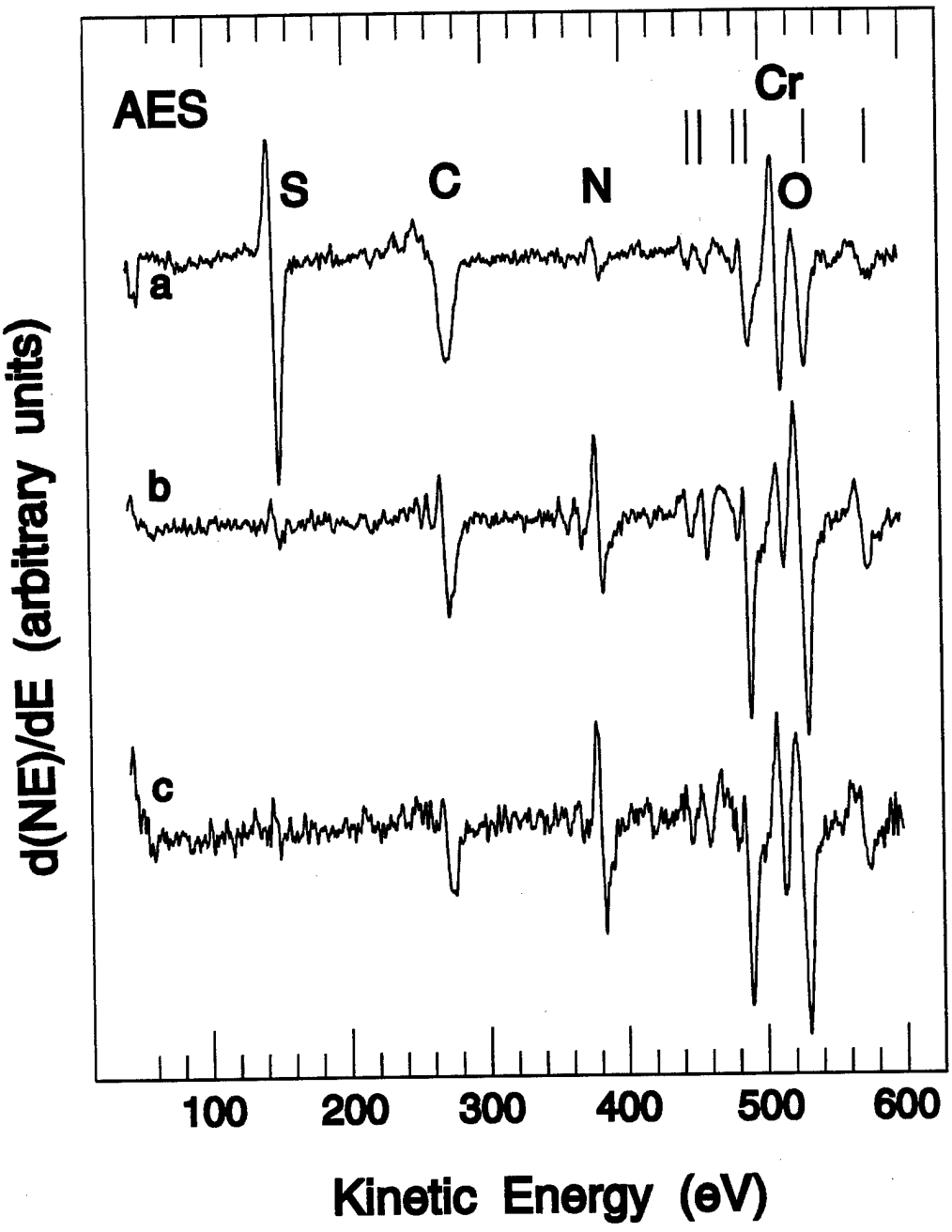

Figure 3-2. Auger spectra taken (a) from the as-prepared ABCD Cr sample annealed at 700°C and N^+ implanted, (b) after Ar^+ sputtering for 75 min and (c) after Ar^+ sputtering for 150 min.

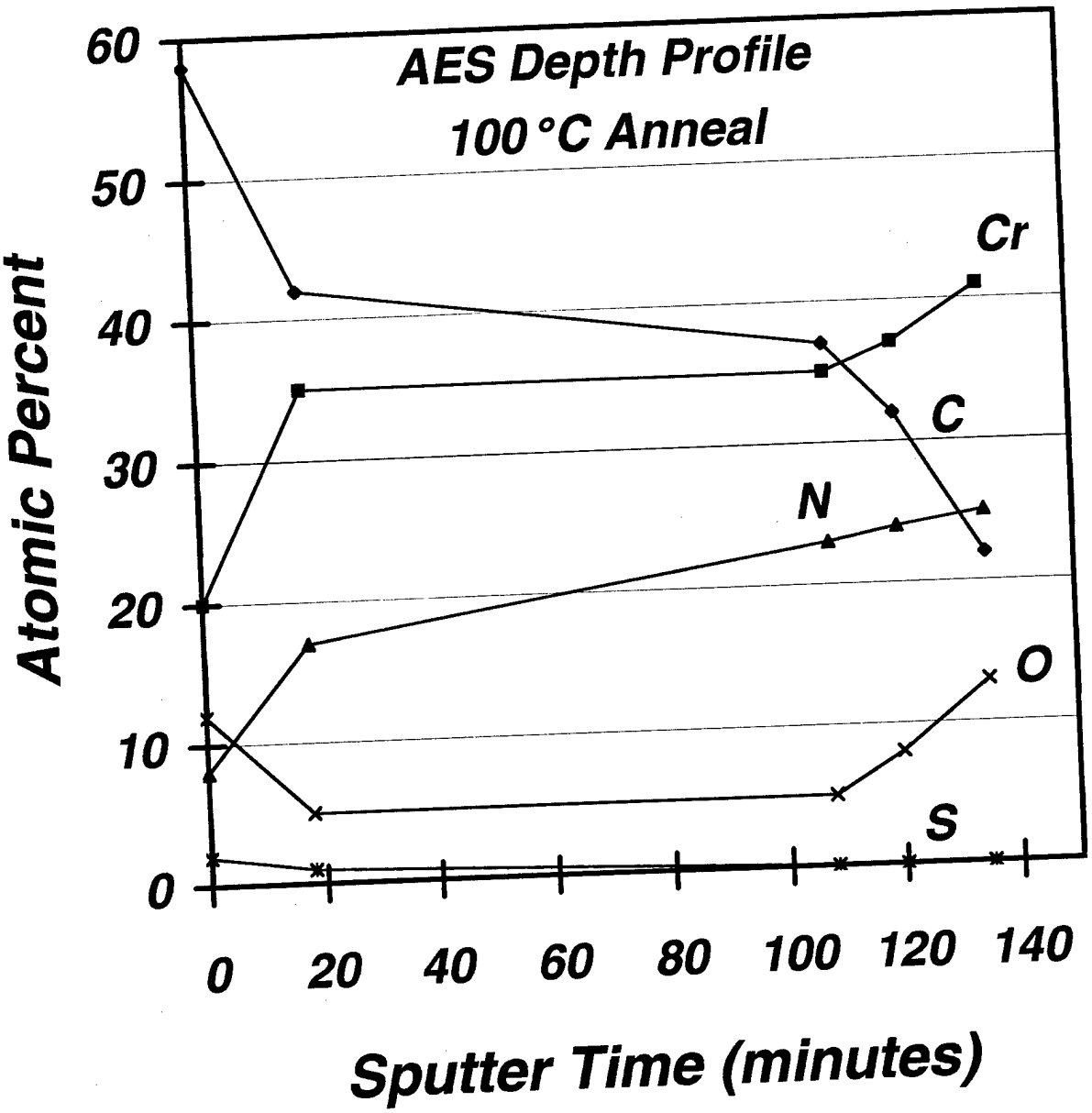

Figure 3-3. Auger composition (atomic %) depth profiles as a function of sputter time for the ABCD Cr film annealed at 100°C and N^+ implanted.

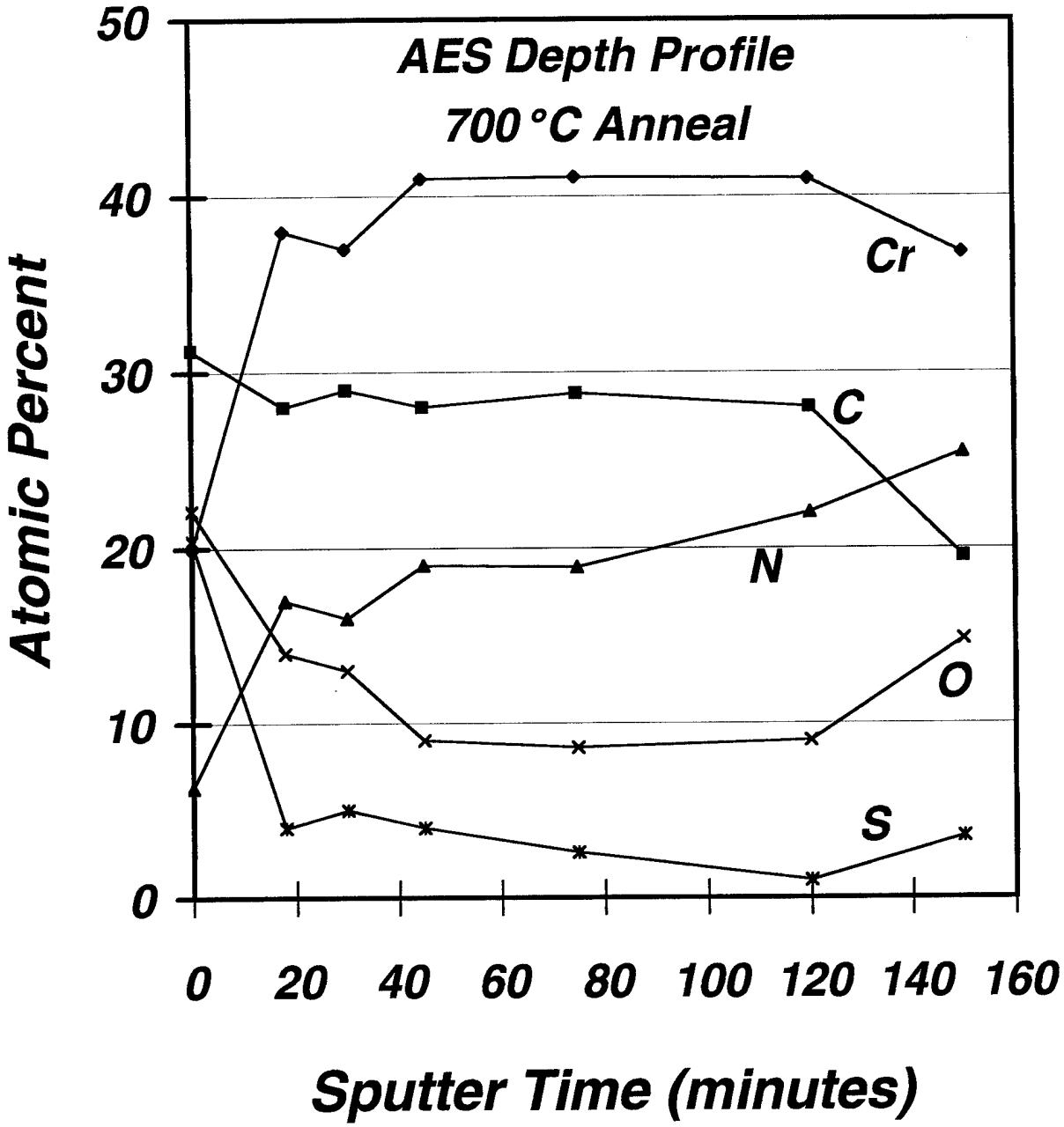

Figure 3-4. Auger composition (atomic %) depth profiles as a function of sputter time for the ABCD Cr film annealed at 700°C and N^+ implanted.

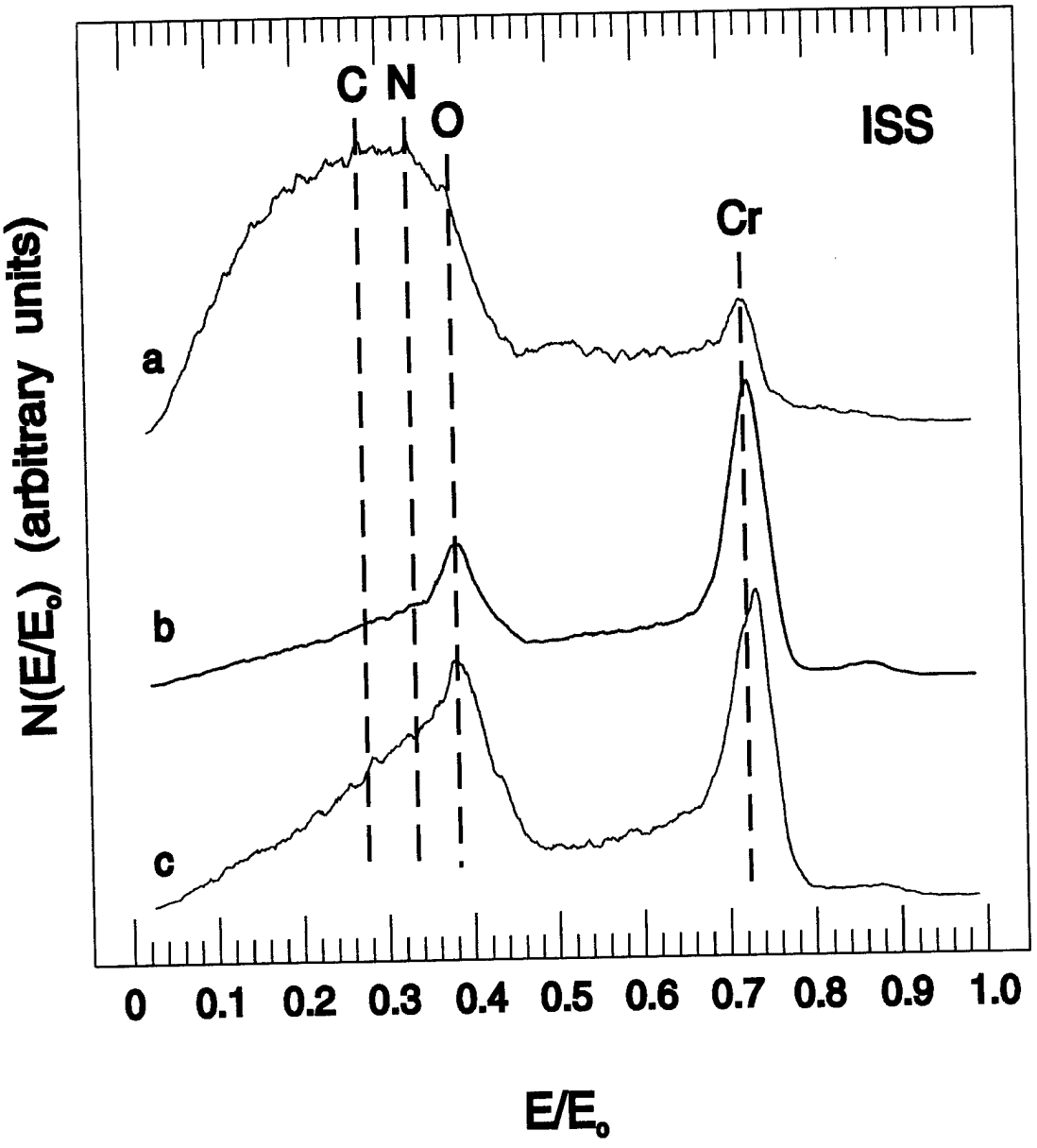

Figure 3-5. ISS spectra obtained from the sample annealed at 100°C and N^+ implanted (a) before sputtering, (b) after Ar^+ sputtering for 15 min, and (c) after Ar^+ sputtering for 135 min.

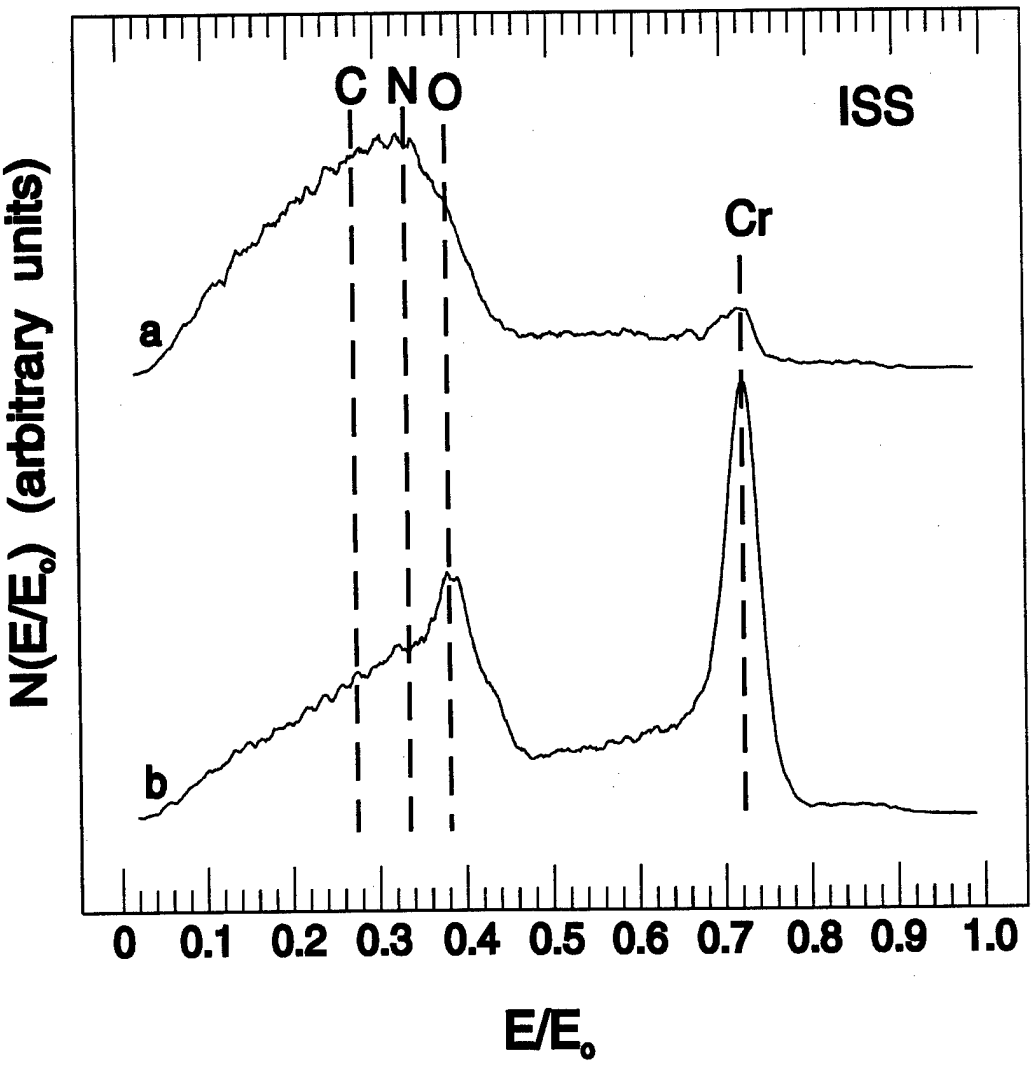

Figure 3-6. ISS spectra obtained from the sample annealed at 700°C and N^+ implanted (a) before and (b) after Ar^+ sputtering for 150 min.

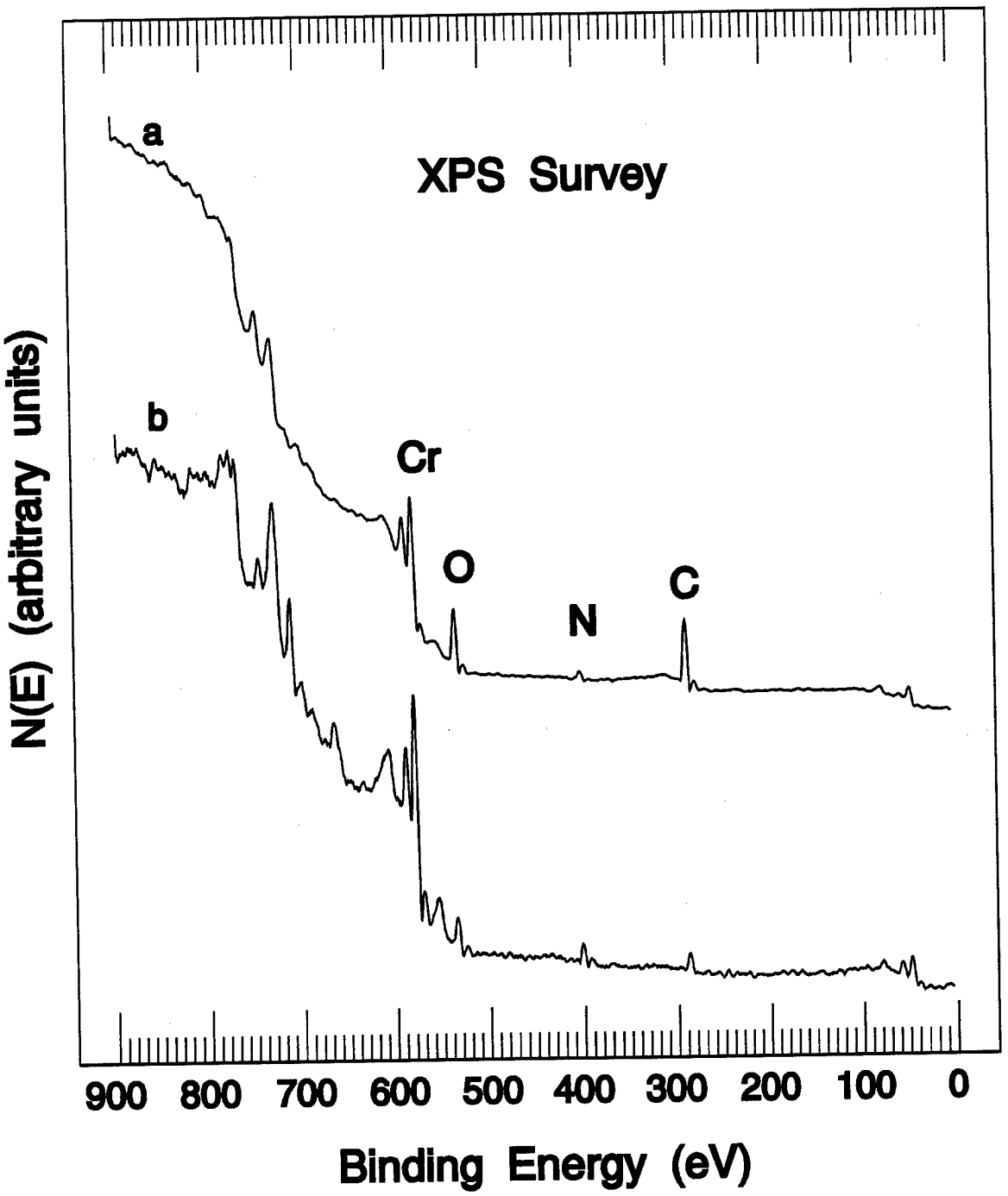

Figure 3-7. XPS survey spectra taken from the ABCD sample annealed at 100°C and N^+ implanted (a) before and (b) after Ar^+ sputtering for 135 min.

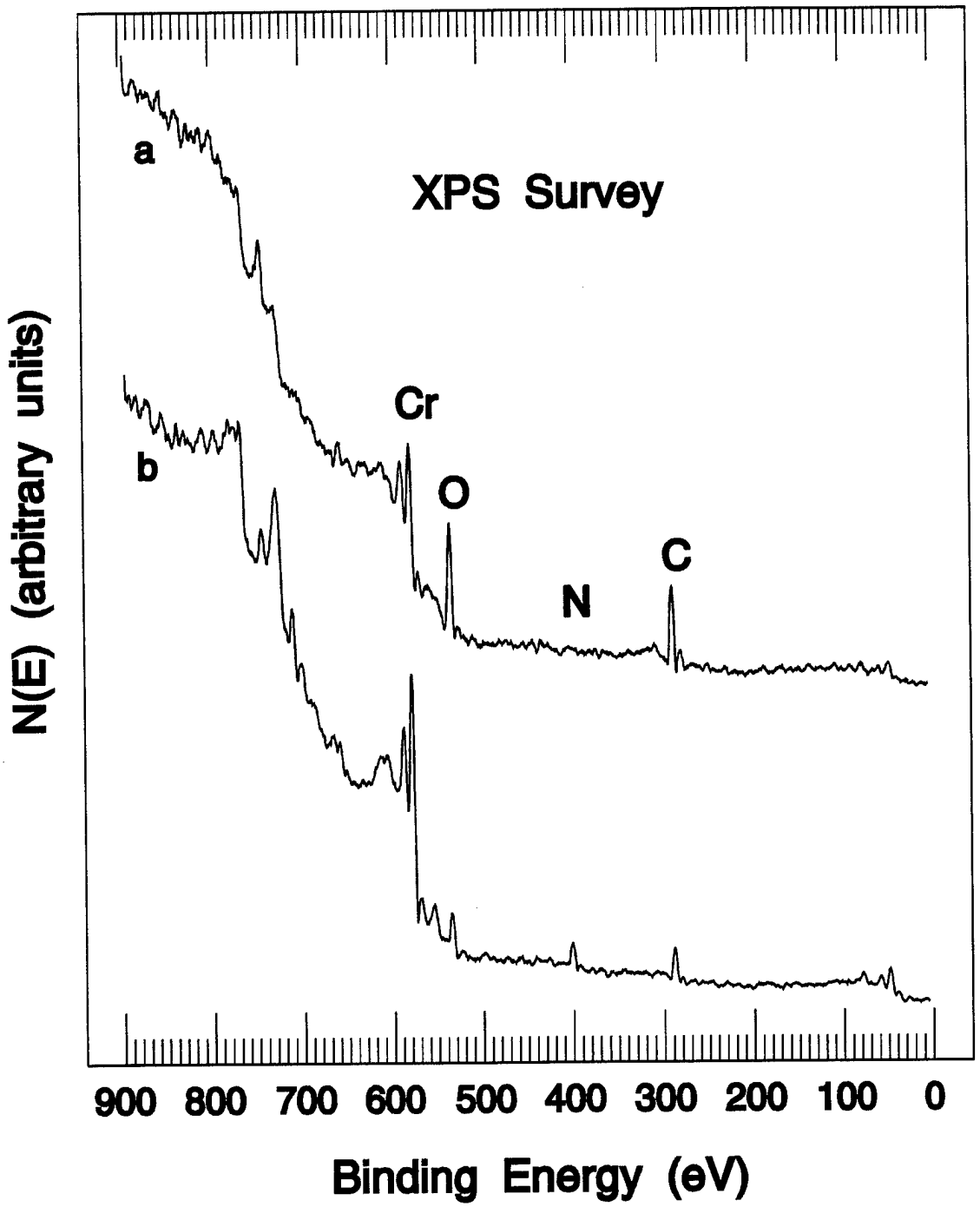

Figure 3-8. XPS survey spectra taken from the ABCD sample annealed at 700°C and N^+ implanted (a) before and (b) after Ar^+ sputtering for 150 min.

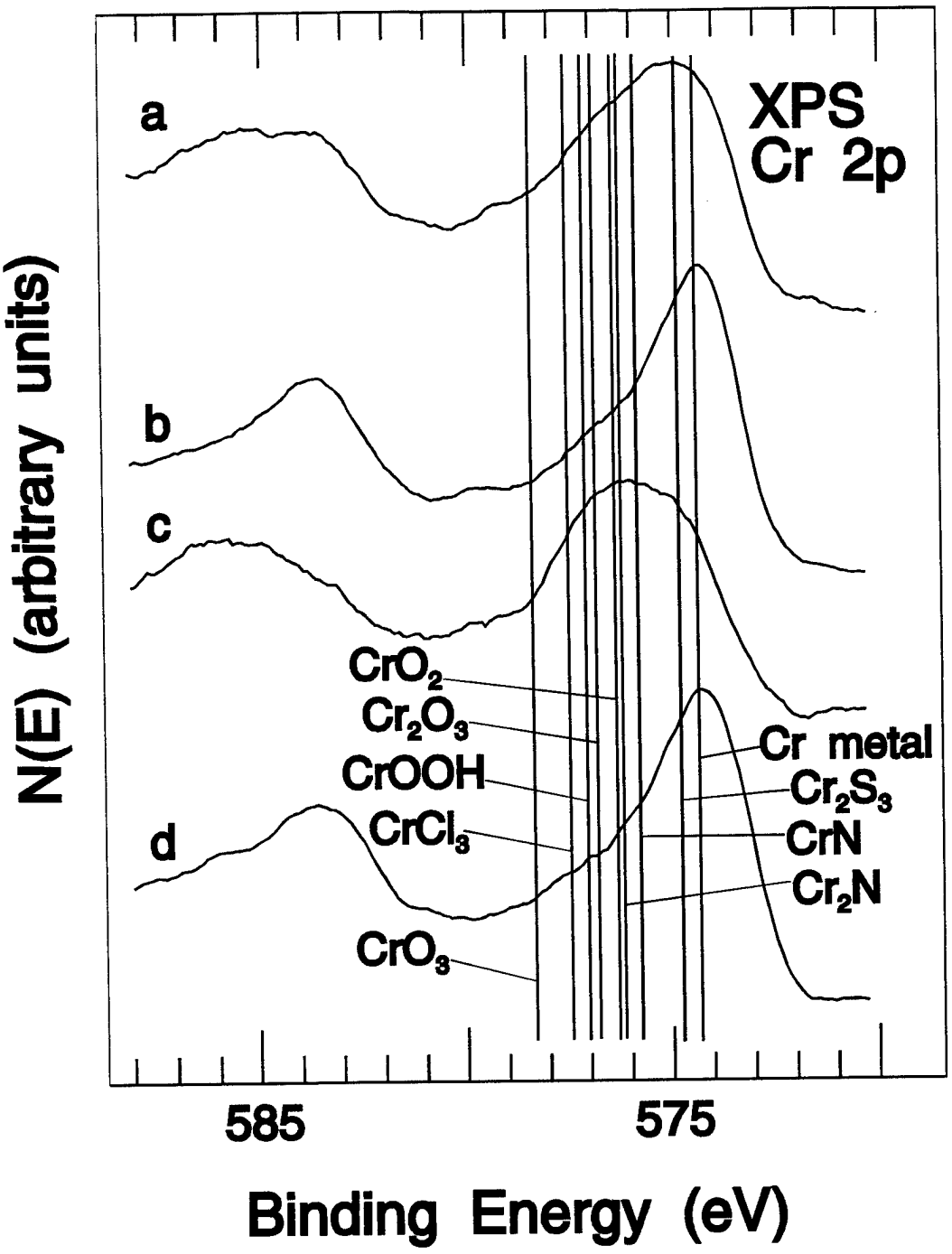

Figure 3-9. High-resolution XPS Cr 2p features obtained from the ABCD sample preannealed at 100°C and N^+ implanted (a) before and (b) after Ar^+ sputtering for 135 min and from the ABCD sample preannealed at 700°C and N^+ implanted (c) before and (d) after Ar^+ sputtering for 150 min.

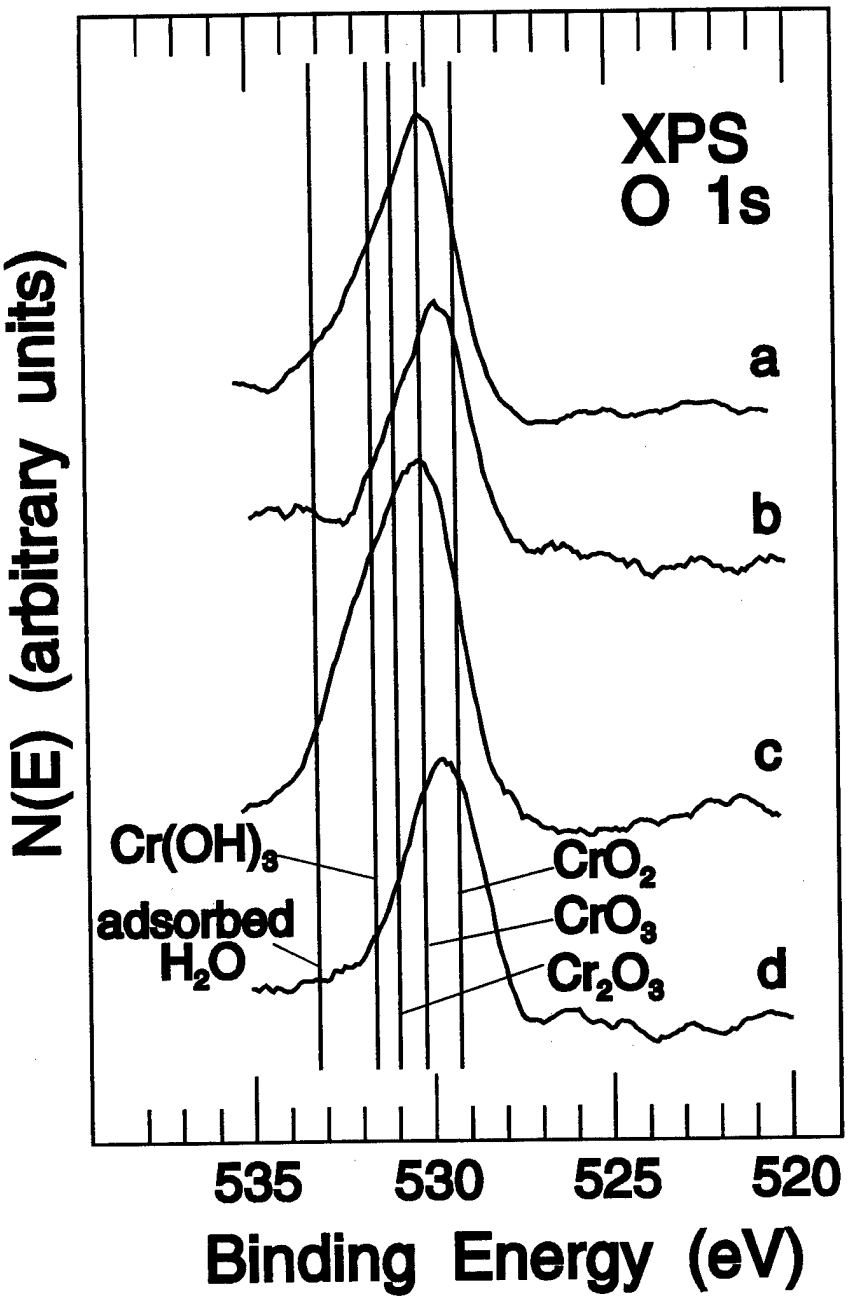

Figure 3-10. High-resolution XPS O 1s features obtained from the ABCD sample preannealed at 100°C and N^+ implanted (a) before and (b) after Ar^+ sputtering for 135 min and from the ABCD sample preannealed at 700°C and N^+ implanted (c) before and (d) after Ar^+ sputtering for 150 min.

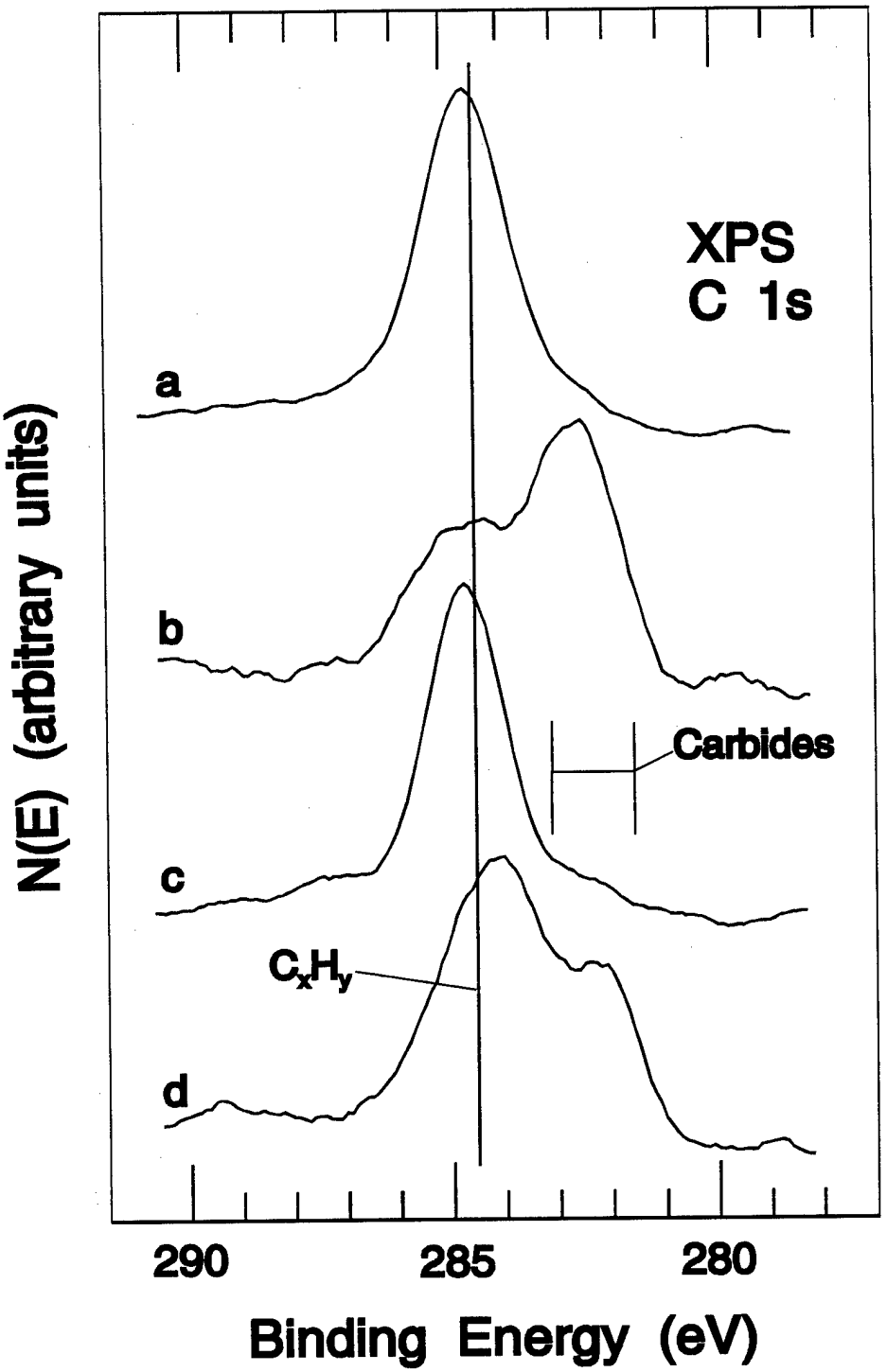

Figure 3-11. High-resolution XPS C 1s features obtained from the ABCD sample preannealed at 100°C and N^+ implanted (a) before and (b) after Ar^+ sputtering for 135 min and from the ABCD sample preannealed at 700°C and N^+ implanted (c) before and (d) after Ar^+ sputtering for 150 min.

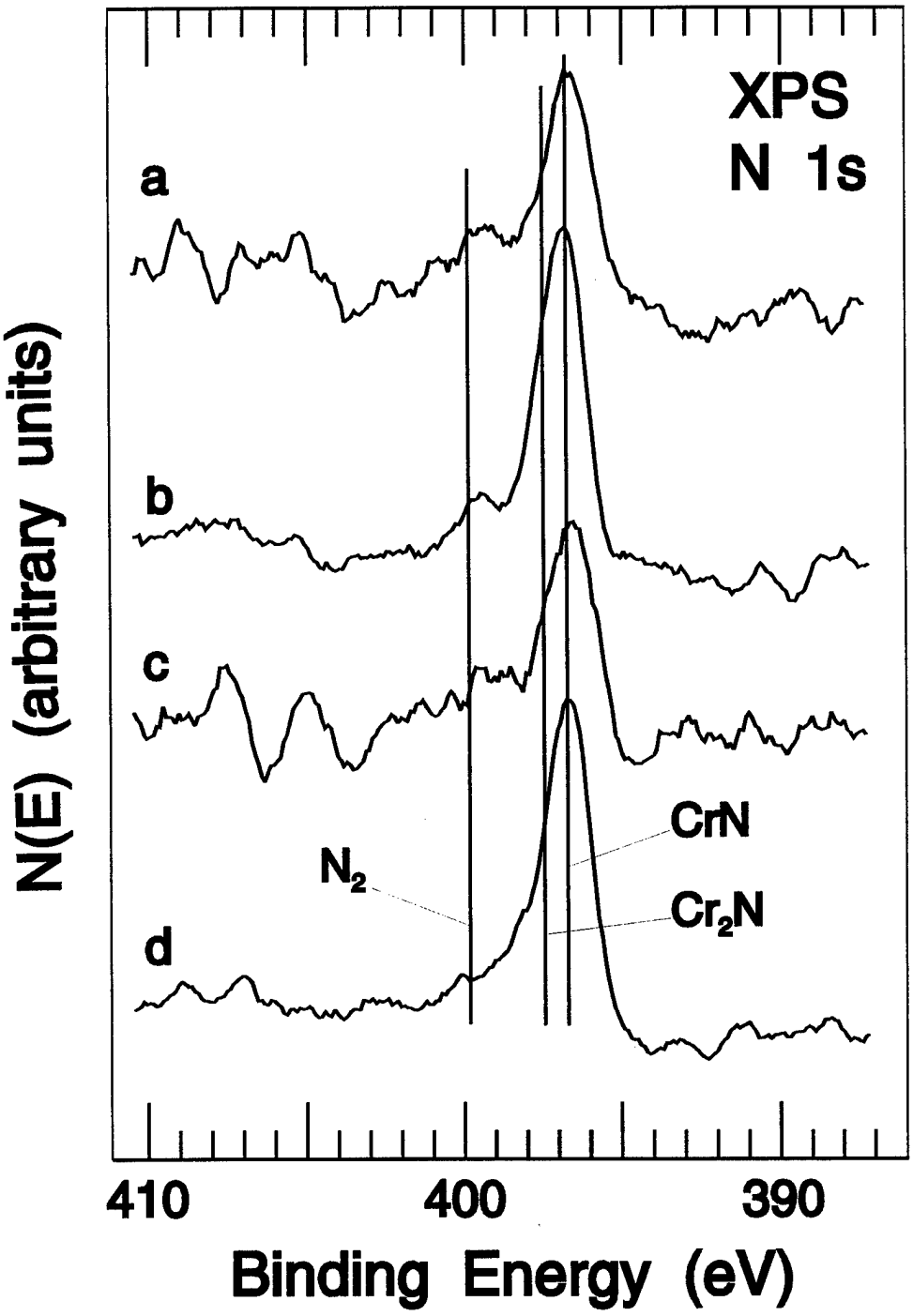

Figure 3-12. High-resolution XPS N 1s features obtained from the ABCD sample preannealed at 100°C and N^+ implanted (a) before and (b) after Ar^+ sputtering for 135 min and from the ABCD sample preannealed at 700°C and N^+ implanted (c) before and (d) after Ar^+ sputtering for 150 min.

CHAPTER 4
PREPARATION OF AMORPHOUS BRIGHT CHROMIUM DEPOSITED FILMS USING PROPIONIC ACID AS ORGANIC ADDITIVE

In 1986 Hoshino, Laitinen and Hoflund (5) described a new method for electroplating amorphous bright chromium deposits (referred to as the ABCD method) from chromic acid solutions containing organic species with -CHO and -COOH groups. Various organic additives have been used on a trial and error basis in the development of this method in order to isolate the one that would yield Cr films with the most desirable properties. Preliminary tests have shown that ABCD films developed with propionic acid as the organic additive in the electroplating bath have superior hardness values and are very bright if plated under the right conditions. Furthermore, the electroplating bath is chemically stable and can be used repeatedly over a period of time to reproduce these films. This chapter outlines the procedure used to develop ABCD films using propionic acid. The films developed from this method will used in future characterization studies continuing a series studies on ABCD films (6-8), conventional Cr films (9) and nitrogen-implanted conventional and ABCD films (10-14).

Preplating Operation

The substrates used were strips of mild steel 9.5 cm x 2.6 cm, 0.3 cm thick. These strips were sanded using sand papers of increasing grit until a mirror shine was produced. Before finishing the sanding process, a metal strip made of tool steel was welded to the substrate. This strip was used to make the connection to the power supply. After sanding, a coating of micro-stop was applied to the backside of the substrate not to be plated.

The substrates were cleaned in an electrolytic cleaner for 2 min cathodically and 1 min anodically with an applied current of 10 Amps (0.4 Amps/cm^2). The electrolytic cleaner had the following composition:

Sodium Hydroxide	35 g/L
Sodium Carbonate	25 g/L
Sodium Lauryl Sulfate	1 g/L
Temperature	70°C

Afterwards the substrates were rinsed in distilled water and immersed in a dilute hydrochloric acid solution for 30 seconds and again rinsed and immediately plated.

Plating Operation

The ABCD chromium layers were deposited in a two step electroplating process. Initially, a conventional chromium layer was deposited from a standard Sargent bath containing 250 g/L of chromic acid and 2.5 g/L of sulfuric acid. In order to ensure proper adhesion between the initial conventional chromium layer and the proceeding ABCD layer it was necessary to deposit the initial conventional chromium layer in such a way as to produce a dull gray finish. This was done by applying a current density of 0.4 A/cm^2 at a temperature of 20°C for 40 min with a 6 cm distance between electrodes. This current density was be attained by means of a gradual increase during the first ten minutes of plating to prevent peeling of the deposited film. The bath was not stirred during plating.

Immediately after depositing the initial conventional chromium film, the PVC plating jig used to hold the sample and the Pb anode in the bath was transferred and immersed into the ABCD plating bath containing 100 g/L of chromic acid, 5 g/L of sulfuric acid and 20 ml/L of propionic acid. The second plating was done applying a current density of 0.4 A/cm^2 at a temperature of 10°C with a distance of 8.5 cm between electrodes

without stirring. The current density was again attained through gradual increase over the initial ten minutes of the 40 min plating session. Under these conditions, at a 15% cathode efficiency calculated from previous experiments, each film was calculated to be 20 μm thick.

The optimum distance between electrodes needed to produce the desired plating was determined through hull cell test experiments. A hull cell is a jig made with prespecified dimensions that holds both electrodes at an angle in order to create a current density gradient. The optimum distance between electrodes can be determined as a function of applied current, current density and the distance along the plated cathode where the desired plating is obtained.

Postplating Operation

After the ABCD layer has been plated the sample is removed from the plating bath thoroughly rinsed in distilled water and annealed at 300°C for 1 hour. This is to allow for better adhesion between the conventional and ABCD layers.

REFERENCES

1. J.F. Moulder, W.F. Stickle, P.E. Sobol and K.D. Bombay, *Handbook of X-ray Photoelectron Spectroscopy*, Perkin-Elmer, Physical Electronics Division, Eden Prairie, MN (1995).

2. L.E. Davis, N.C. MacDonald, P.W. Palmberg, G.E. Raich and R.E. Weber, *Handbook of Auger Electron Spectroscopy*, Perkin-Elmer, Physical Electronics Division, Eden Prairie, MN (1979).

3. G.J. Sargent, *Trans. Am. Electrochem. Soc.* 37(1920)479.

4. C.G. Fink, US Patent 1,581,188 (1926).

5. S. Hoshino, H.A. Laitinen and G.B. Hoflund, *J. Electrochem. Soc.* 133(1986)681.

6. G.B. Hoflund, D.A. Asbury, S.J. Babb, A.L. Grogan, Jr., H.A. Laitinen and S. Hoshino, *J. Vac. Sci. Technol.* A 4(1986)26.

7. G.B. Hoflund, A.L. Grogan, Jr., D.A. Asbury, H.A. Laitinen and S. Hoshino, *Appl. Surface Sci.* 28(1987)224.

8. S. Hoshino, S. Nakada, C.K. Mount and G.B. Hoflund, *Proc. Amer. Electro. Surface. Fin. 80th Ann. Tech. Conf.* K(1993)471.

9. G.B. Hoflund, M.R. Davidson, E. Yngvadottir, H.A. Laitinen and S. Hoshino, *Chem. Mater.* 19(1989)625.

10. H. Ferber, G.B. Hoflund, C.K. Mount and S. Hoshino, *Surface and Inter. Anal.* 16(1990)448.

11. H. Ferber, G.B. Hoflund, C.K. Mount and S. Hoshino, *Nucl. Instrum. Meth. Phys.* Res. B 59/60(1991)957.

12. H. Ferber, C.K. Mount, G.B. Hoflund and S. Hoshino, *Thin Solid Films* 203(1991)121.

13. H. Ferber, C.K. Mount, G.B. Hoflund and S. Hoshino, *Surf. Coat. Technol.* 51(1992)313.

14. G.B. Hoflund, C.K. Mount, R.I. Gonzalez, H. Ferber, G. N. Salatia and S. Hoshino, *Thin Solid Films*, in press.

15. Y. Nonaka, K. Saito, T. Inoue and S. Hoshino, *Thin Solid Films*, in press.

BIOGRAPHICAL SKETCH

Rene I. Gonzalez Rodriguez was born on March 4, 1974, in Santurce, Puerto Rico, to Rene A. Gonzalez Freyre and Juanita F. Rodriguez Aleman. At the age of 4, his mother remarried to Francisco Rodriguez Rivera, and Rene and his family moved to Spain where he lived until the age of 15. Rene then moved back to Puerto Rico where he resided with his uncle, Jose I. Gonzalez Freyre, while attending high school at the Baldwin School of Puerto Rico, graduating in 1992. Rene began his college education at Rensselaer Polytechnic Institute in September of 1992 in Troy, New York. In May 1996 he graduated with his Bachelor of Science in chemical engineering and was commissioned as a Second Lieutenant in the United States Air Force. Sponsored by the Air Force, Rene decided to return to college as a graduate student in chemical engineering at the University of Florida where he performed research for Dr. Gar B. Hoflund in surface science and chromium films.